

Advanced Sustainable BIOfuels for Aviation

Deliverable D2.8: R&D on pre-treatment report

Consortium:

Acronym	Legal entity	Role
RE-CORD	CONSORZIO PER LA RICERCA E LA DIMOSTRAZIONE SULLE ENERGIE RINNOVABILI	CO
TRC	TOTAL RAFFINAGE CHIMIE SA	BEN
TRF	TOTAL RAFFINAGE FRANCE	BEN
SKYNRG	SKYENERGY BV	BEN
CENER	FUNDACION CENER-CIEMAT	BEN
ETA	ETA – Energia, Trasporti, Agricoltura Srl	BEN
CCE	CAMELINA COMPANY ESPANA S.L.	BEN
JRC	JOINT RESEARCH CENTRE – EUROPEAN COMMISSION	BEN

CO...Coordinator, BEN...Beneficiary

'The sole responsibility for the content of this report lies with the authors. It does not necessarily reflect the opinion of the European Union. The European Commission is not responsible for any use that may be made of the information contained therein.

This project has received funding from the European Union's Horizon 2020 research and innovation programme under grant agreement No. 789562.



General Information

Call identifier: H2020-LCE-2017-RES-IA
 GA Number: 789562
 Topic: LCE-20-2016-2017
 Start date of project: 01/05/2018
 Duration: 4 years (30/04/2022)
 Work Package: WP2 - R&D Long Term Strategy for HEFA production
 Type: Deliverable
 Number: D2.8
 Title: R&D on pre-treatment report
 Due Date: 31/10/2020 (Month 30)
 Submission date: 31/10/2020
 Reference Period: 01/05/2018 – 31/10/2020
 Prepared by: Marco Buffi (Lead), Ramin Magrebi, Tommaso Barsali, David Chiaramonti
 Responsible Person: Marco Buffi
 Dissemination Level: Public

INTERNAL MONITORING & REVISION TABLE

REV.	DATE	DESCRIPTION	PAGES	CHECKED	APPROVED
1	21/10/2020	Original	50	TB	XXX
2	30/10/2020	Final version	50	TB	DC

Document Type

PRO	Technical/economic progress report (internal work package reports indicating work status)	X
DEL	Technical reports identified as deliverables in the Description of Work	
MoM	Minutes of Meeting	
MAN	Procedures and user manuals	
WOR	Working document, issued as preparatory documents to a Technical report	
INF	Information and Notes	

Dissemination Level

PU	Public	X
PP	Restricted to other programme participants (including the Commission Services)	
RE	Restricted to a group specified by the consortium (including the Commission Services)	
CO	Confidential, only for members of the consortium (including the Commission Services)	
CON	Confidential, only for members of the Consortium	



Table of Contents

Table of Contents	4
1. Summary	5
2. Introduction	6
3. Literature review	7
3.1 Feedstock	7
3.2 Conversion to biofuels	7
3.2.1 HVO process	8
3.2.2 Direct catalytic and non-catalytic conversion of lipids in hydrocarbons.....	8
4. R&D initial work and equipment	27
4.1 Catalytic pyrolysis unit	28
4.2 Hydrothermal liquefaction unit	28
5. Experimental campaign: materials and methods	30
5.1 Feedstock and methods of analysis	30
5.2 Experimental apparatus	32
5.3 Methods for MRTB tests, collection of product and titration	34
5.3.1 Deoxygenation tests	34
5.3.2 Hydrolysis tests	34
5.3.3 Sample collection.....	35
5.3.4 Titration	35
5.4 Design of experiments	36
6. Experimental campaign: results	37
6.1 Feedstock	37
6.2 Hydrolysis tests	37
6.3 Deoxygenation tests	39
6.3.1 Effect of reaction temperature and heating rate	40
6.3.2 Conversion yield	41
6.3.3 Acidity and deoxygenation degree	43
6.3.4 Hydrocarbons quantification	44
6.3.5 Discussion	45
6.3.6 Conclusions	46
6.3.7 Bibliography/References	48

1. Summary

The research and demonstration activities regarding UCO, residual lipids and fatty acids pre-processing is the main object of the present deliverable. A brief overview of the ongoing activities has been introduced in the progress report at M18, but just preliminary results have been reported. The target of the present Bio4A' task is mainly related to experimental lipids pre-treatment before HRJ production, focusing on a preliminary deoxygenation of feedstock to save hydrogen demand into the next processing step. The R&D activities started with a preliminary literature review addressed to the state-of-the-art of waste lipids processing to advanced biofuels, in particular re-elaborating the experience of RE-CORD collected in scientific publications and thanks to EU FP7 ITAKA project. As main outcome it was demonstrated that lipids upgrading is possible (producing a considerable amount of renewable hydrocarbons), but several oxygenated chemical species were still present into the process product.

Considering that HVO process requires high flow rates of H_2 at high pressures and the use of expensive catalysts to favor the hydro-deoxygenation reaction, the scope of this task focuses on the experimental demonstration of a direct deoxygenation of the triglycerides, which are the main UCO constituent as feedstock pre-treatment. A thermochemical process which does not require hydrogen could be considered as very promising since it allows an overall saving in energy conversion demand to renewable hydrocarbons.

The existing demo-units at RE-CORD facilities, such as a modified pyrolysis unit of 1.5 kg h^{-1} capacity, generated a too much intense cracking performance to perform the only deoxygenation reaction, thus more R&D efforts at lab scale are necessary for the present R&D pre-conversion step before commercial HVO.

Through a deep literature review, the elemental bond energies were studied and a set of experiments was performed to investigate the selected deoxygenation reaction (i.e. direct decarboxylation). The target is to directly convert a molecule of stearic acid into one heptadecane and one carbon dioxide molecules.

The experimental campaign started with hydrolysis of glycerol trioleate (one of the main constituents of UCO) at $230 \text{ }^\circ\text{C}$, 40 bar as initial pressure, and a reaction time of 2 hours. The hydrolysis reaction partially occurred and demonstrated the production of free fatty acids.

Then, direct non-catalytic deoxygenation tests were carried out in a temperature range between 300 and $470 \text{ }^\circ\text{C}$ in a batch experimental reactor of 42 ml. Each test had the following fixed parameters: reaction time of 30 minutes; initial pressure of 0.1 bar; inert ambient of N_2 ; a content of 13.7 g of stearic acid. The results showed that the most performant deoxygenation reaction happened at $450 \text{ }^\circ\text{C}$, with high fractions of hydrocarbons (mainly heptadecane) collected into the liquid product.

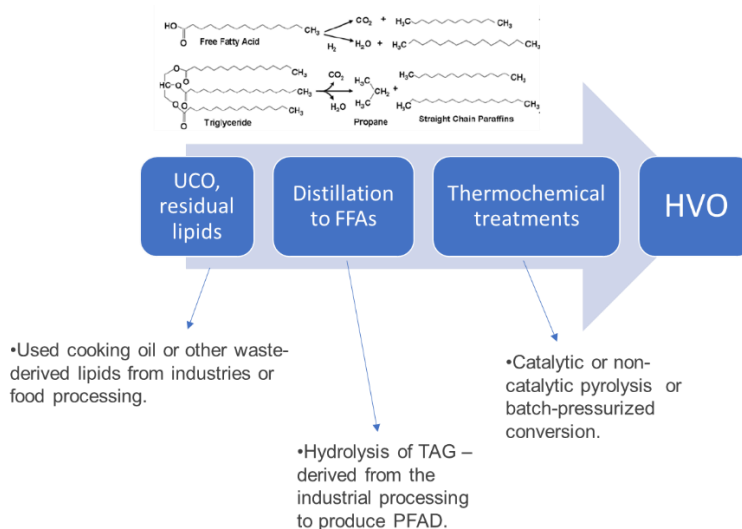


Figure 1: A scheme of the proposed R&D pre-treatment for waste lipids before HVO.



2. Introduction

In the last years, the European Commission is promoting the use of advanced biofuels, which can be obtained from non-edible cultivation or waste products. Some of these biofuels are Dimethyl ether (DME), biogas or biomethane, Hydro treating Vegetable Oil (HVO) and Fischer Tropsch fuels (FT fuels). In particular, HVO production has been developing rapidly. More and more major oil companies, such as ENI or Total, have started investing in HVO production units. This growth of production is due to the high quality of the HVO and its properties since it is composed by only renewable hydrocarbons: it can be considered as a drop-in fuel to be used in an internal combustion engine without limits. In addition, it does not contain any sulfur or aromatics. Despite its excellent production, the HVO process requires high flow rates of H_2 at high pressures, and the use of expensive catalysts to allow the hydrodeoxygenation reaction.

Consequently, the objective of this work focuses on the experimental demonstration of an alternative pathway, that could be even used as a pre-treatment for HVO, to produce bio-hydrocarbons through the direct deoxygenation. The process targets to remove the oxygen atoms from triglycerides or fatty acids to obtain normal paraffin hydrocarbons as final product. In order to remove the oxygen atoms, a single thermal cracking reaction was studied. The main factor of influence is the process temperature, but even pressure, heating rate, initial feedstock, reaction time and type of reactor have a significant impact on the final product. For example, unsaturated fatty acids as initial feedstock strongly influenced the reaction: the presence of a double bond in the hydrocarbon chain weakens the adjacent C-C bonds and increases the possibility that the first breakage occurs in these points, or in any case it occurs at the same time of other breakages. This is an unwanted condition since it can obtain more short chain hydrocarbons. Therefore, many authors in literature carried out numerous experiments with saturated fatty acids for the absence of a double bond, which should favour an easier separation of the carboxylic group from the hydrocarbon chain. These pathways will be investigated in the next chapter.

The scope of the present work is to obtain long chain hydrocarbons (in particular heptadecane C17) through direct deoxygenation of stearic acid to demonstrate a feasible and economically viable upgrading strategy of lipids wastes before commercial HVO process.

Therefore, a set of experiments was carried out in RE-CORD laboratory in a batch reactor of 42 ml. Chapter 3 studied the literature behind the present proposed conversion pathways. Chapter 4 and 5 investigated the RE-CORD' experimental equipment available and used for tests. Chapter 6 investigated the results at M30 of the proposed R&D strategy to upgrade waste lipids-derived feedstock.

3. Literature review

3.1 Feedstock

Waste cooking oil (WCO) consists in a mixture of edible vegetable oils, and sometimes animal fats, which mainly derive from fried food. The use of WCO is the most inherent example of circular economy. Without reclamation facilities waste cooking oils and fats can give rise to significant disposal problems and in doing so create odour and pollution [1]. According to the Energy Information Administration (EIA) the USA's annual production is around 378,000 m³ and European Union production about 700,000 to 1,000,000 tons per year [2], while 5 million tons of waste cooking oil (WCO) is produced each year in China [3] (the most important source of used vegetable oil waste are restaurants, hotels, school cafeterias, hospitals and refectories) and up to now: only 20 % (around 35 million tons/year) of these used oils are valorized [4]. So addressing this waste disposal problem to create a fuel substitute can potentially offer both economic and environmental benefits. Many developed countries have outlawed the disposal of waste cooking oil in the domestic drainage system [5]. The major factors inhibiting the utilization of this technology for biofuels production are the non-uniform value of the acid index, the solids content, the need for heavy equipment for large-scale production, and the alcohol required for the recovery and purification (in case of transesterification) [6].

The composition of used frying oils partially differs from the corresponding fresh oils (some difference can also be seen in Figure 2), but the results obtained after the thermal treatment are identical to those obtained from treated fresh oils in term of liquid yield hydrocarbon content. Sannita et al [7] report many results in terms of comparisons between fresh oils and exhausted oils (sunflower oil, palm oil, etc.): generally, in WCO, an increase in density is observed, an increase in the sulfur (most likely resulting from the food) and nitrogen contents (also derived from food or possibly from the nitrogen present in the air); moreover the total concentration of unsaturated fatty acids increase in the used oil, whereas the palmitic and oleic acid contents decrease and the contents of stearic and linoleic acid increase. In the case of the frying process this is due to the interaction between oil and food which cause several reactions like: hydrolysis, polymerization, oxidation, and in some cases cyclization of the fatty acids [2,7]. Finally, Sannita et al conclude that adding waste oils to fresh oils during the pyrolysis process does not impart significant variations in the process itself. The only observed change was a slight difference in the amount and quality of liquid/gaseous products.



Figure 2: Different appearance between, palm oil, WCO and biodiesel [8].

The most common utilization of WCO is for fuel production by esterification and/or transesterification to produce biodiesel. In detail, approximately 80-90 % of the WCO collected in the EU is used for biodiesel production, and the other fraction for energy and oleochemicals; just a small quantity is directed to other uses.

3.2 Conversion to biofuels

At commercial scale, thermochemical conversion of lipids is generally divided into two big categories: the first is the biodiesel industry, which produces an ester suitable for blending with fossil diesel fuel up to defined fractions; the second is the HVO (Hydrotreated Vegetable Oil) industry, which produces a full hydrocarbon fuels suitable as drop-in fuels for aviation and road transport sectors. At experimental level, scientific literature went through a third category, which is the direct catalytic and non-catalytic conversion of lipids in hydrocarbons. This paragraph reports a detailed chemical investigation of the reaction studied within T2.3.

3.2.1 HVO process

BIO4A involves TOTAL' HVO process, that consists in the conversion of lipids in green hydrocarbons through various catalytic reaction mechanisms in presence of hydrogen. The scope is to saturate the double bonds present into the triglycerides through hydrogen addition in a reactor at certain temperatures and pressures. The reaction is known as "hydrogenation", that means a completely conversion of all unsaturated fatty acids in saturated ones (shown in Figure 3). Therefore, after saturation, more hydrogen addition causes the breaking of glycerol, forming propane and free fatty acids; the carboxylic acid group that remains attached to the free fatty acid is consequently removed to form straight chain alkanes "hydrodeoxygenation reaction" [9].

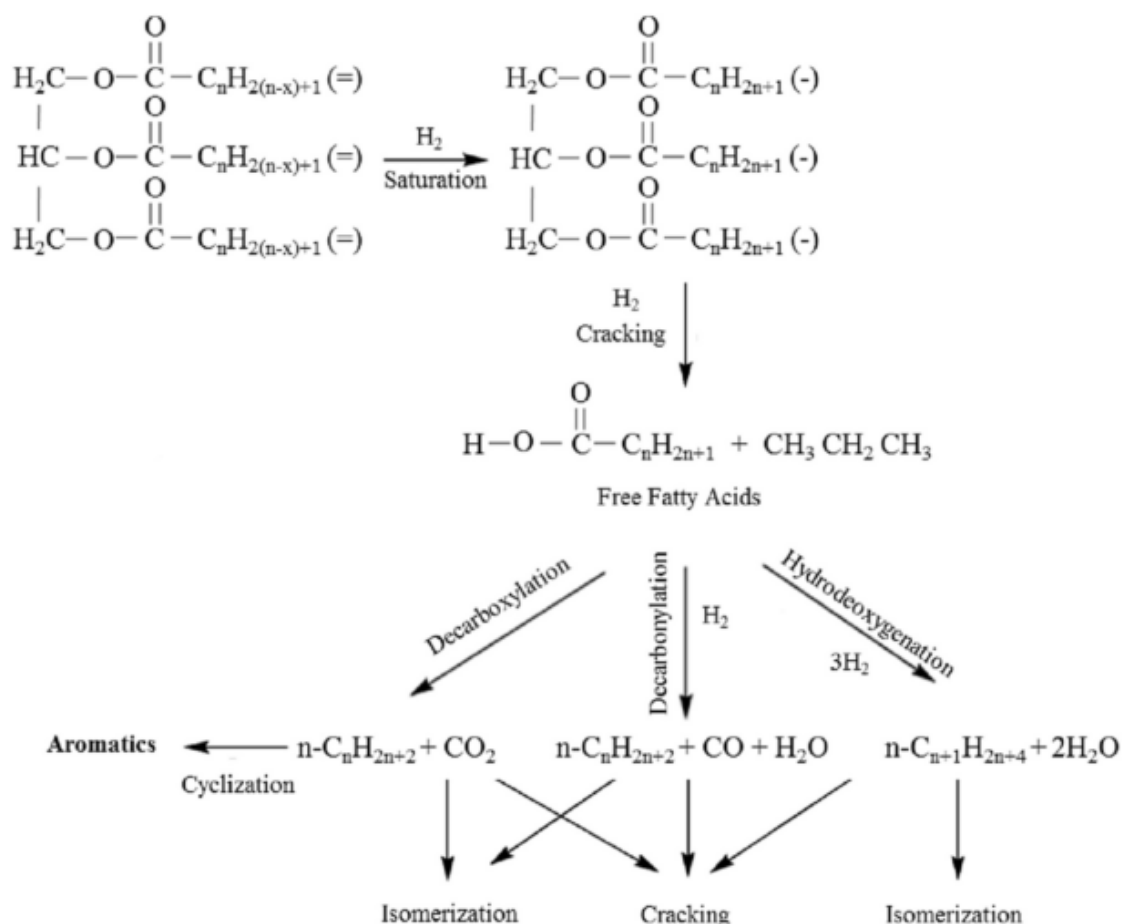


Figure 3: Conversion of a triglyceride molecule under catalytic hydrotreatment [9].

Since hydroprocessing can use a wide range of waste fats and oils as feedstocks, the synonym HEFA (Hydroprocessed Esters and Fatty Acids) is more appropriate. Despite its high quality, the process requires the use of pure hydrogen, which comports relevant costs (e.g. hydrodeoxygenation – HDO - needs more than 300–420 m³ of hydrogen for one m³ of oil to remove the oxygen as H₂O [10]). Therefore, hydroprocessing requires high H₂ pressures, and conventional hydrotreating catalysts consist

of metal sulfides that require careful handling and risk of sulfur contamination [11,12]; all this makes the process sustainable only in large industrial facilities like refineries, where the availability of hydrogen is facilitated. In recent years, other companies apart Total, such as Neste Oil, Honeywell and ENI, started the commercial production of HVO, both for road and air transport fuels [11].

3.2.2 Direct catalytic and non-catalytic conversion of lipids in hydrocarbons

A promising alternative to convert lipids in pure hydrocarbons is the direct thermal conversion of lipids (with the potential presence of catalysts) in hydrocarbons. Reaction mechanisms are similar to traditional pyrolysis, but a pressurized environment could be applied to the process. The process has been deeply studied in literature and it can be conducted either with or without a catalyst, at temperatures ranging from 300 to 800 °C. A higher amount of light products, including gases and compounds with a high degree of deoxygenation, generally are the contained into the liquid product when higher temperatures or when catalysts occur. The nature of the fatty compounds also influences the composition of the products. If pressurization of reactor is not applied, the pyrolysis of triglycerides and fatty acids at 400–500 °C leads to rather complex liquid products and only moderate yields of deoxygenated compounds [13].

This process targets the specific deoxygenation of fatty acids via three main reaction pathways, as shown in Figure 4.

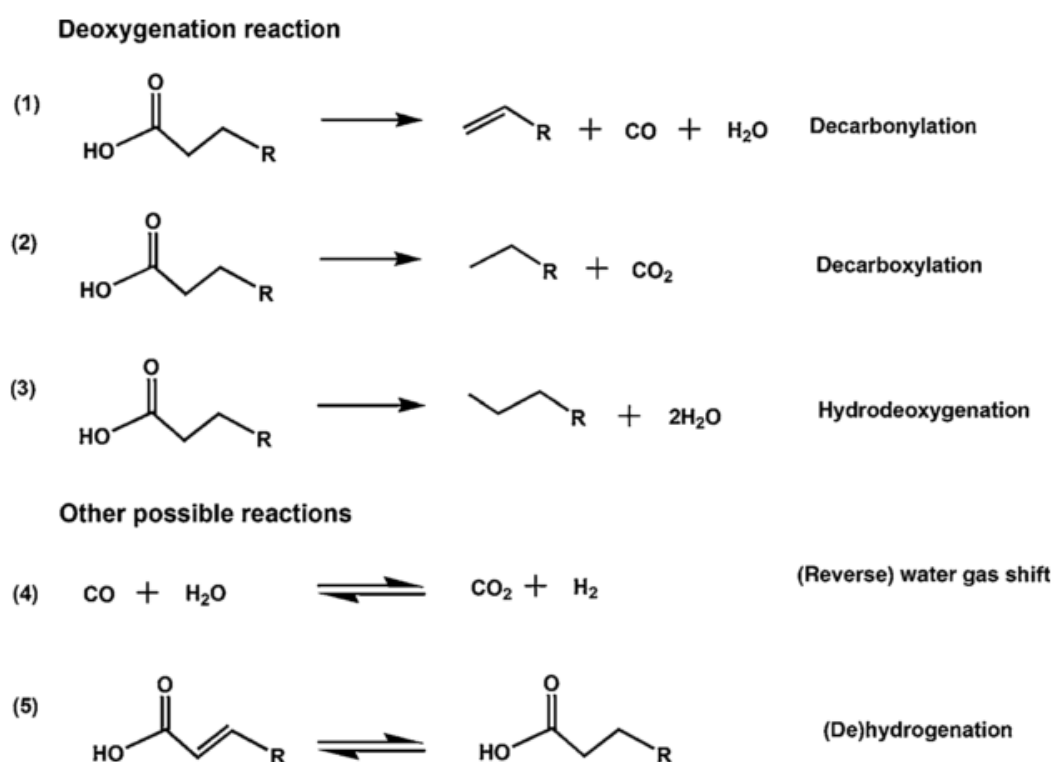


Figure 4: Pathways for the deoxygenation of a fatty acid ester into hydrocarbons [14].

As reported by Krobkrong et al [15], decarbonylation (DCO) and decarboxylation (DCO₂) yield straight chain alkanes with shorter hydrocarbon chains than that of the original fatty acid and the by-products for those two reactions are CO and water and CO₂, respectively. The DCO and DCO₂ reactions are more practical as they can be operated under mild conditions with low amount of H₂, even accounting for the unintentional CO₂/CO hydrogenation (methanation reaction) which could occur under the conventional conditions of deoxygenation. As already mentioned, hydrodeoxygenation (HDO) produces a straight-chain alkane which retains the hydrocarbon chain length of the original fatty acid and produces a water by-product, but consuming the highest amount of H₂ (at high pressure) in comparison to the others, leading to the high cost and serious concerns for equipment, safety, operations, etc. These reaction mechanisms explain how the fatty acids chains break down, but which reaction products are obtained is not yet well-known.



To understand the main mechanisms that happen during the pyrolysis process, Khorasheh and Gray [16] did a thermal cracking of n-hexadecane (n-C₁₆); being the feedstock only a hydrocarbon it was easier to analyse and to understand its reaction mechanism. Figure 5 shows the possible steps of the reaction mechanism for high-pressure thermal cracking of n-C₁₆:

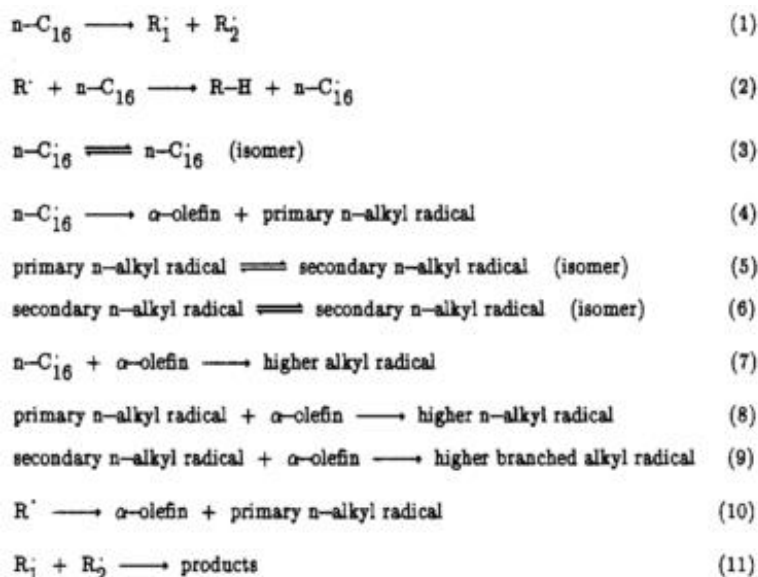


Figure 5: Reaction mechanism for high-pressure thermal cracking of n-C₁₆ [16].

Regarding the benefits of exploiting high pressures, Khorasheh and Gray [16] went even beyond and developed a kinetic model on the basis of their theory of free-radical mechanism for thermal-cracking process at mild temperatures and high pressures which was in agreement with the experimental data. They revealed the advantage of high-pressure thermal cracking in higher percentage of saturated products. They proposed the justification of this advantage as follows.

1. The long chain hexadecane is cracked two radicals
2. Every radical then can be cracked to another radical and an unsaturated compound
3. Thanks to the high-pressure which is higher than saturation pressure of unsaturated compounds from step 2 unsaturated compounds are kept in the liquid phase along with radicals; and thanks to very low activation energy of 2-8 kcal/mol for radical addition reactions, a radical is added to an unsaturated compound and produces either saturated linear compounds or saturated branched compounds.

Another advantage of high-pressure cracking can be minimizing the cyclization and aromatization reactions (Figure 6). This can be justified by le chatelier's principle. In particular, high pressure shifts both reactions towards left. In this way, final products will predominantly contain saturated alkanes.

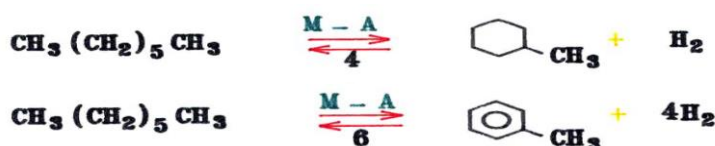


Figure 6 Aromatization and cyclization [17]

Concerning triglycerides, some authors [4,18–20] report the studies done by Chang and Wang [21] on thermal cracking of vegetable oils: they proposed a first scheme of 16 types of reaction for the triglyceride decomposition. The cleavage of triglycerides molecules originates a mixture of hydrocarbons of smaller chains and oxygenated compounds, such as alkanes, alkenes, alkadienes, aromatics, aldehydes, ketones, and carboxylic acids. Prado and Filho [22] and Chiaramonti et al [19] report of a mechanism based on a two-step cracking system that occurs simultaneously:

1. Primary cracking: acid species (mainly carboxylic acids) are formed during the thermal decomposition of triglycerides by means of the breakdown of C-O bonds of the carboxylic group.

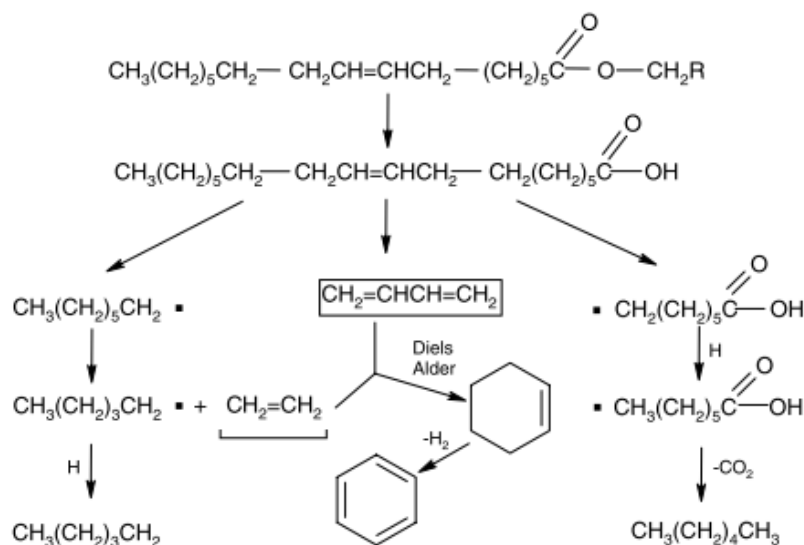
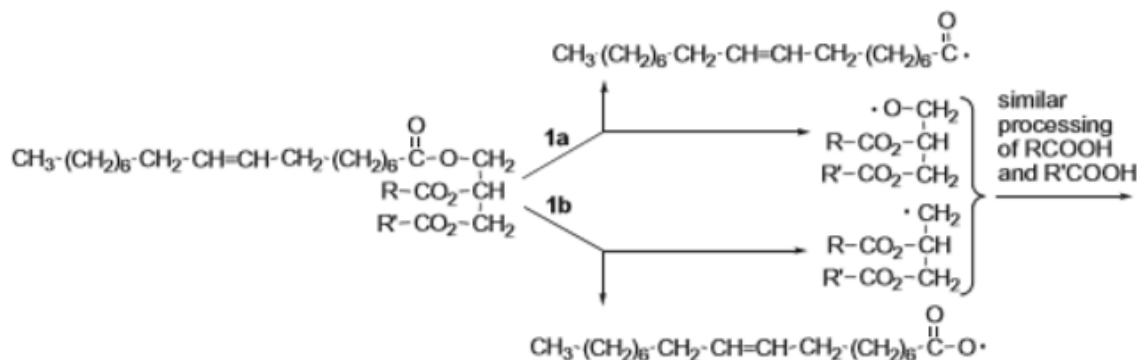


Figure 8: Thermal cracking scheme of an unsaturated triglyceride [24].

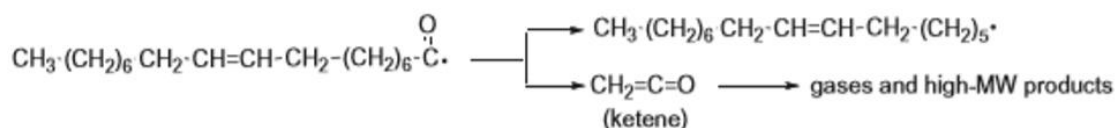
According to this mechanism, in the first step, an unsaturated fatty acid radical is separated from a triglyceride molecule and then it is cracked along its carbon chain before a carboxyl group, which results in smaller fatty acid radicals form paraffinic and olefinic hydrocarbons. Fatty acid radicals absorb hydrogen atoms and will be converted into a molecule. Then a CO_2 molecule will be removed and an alkane will form. Another recommendation of this mechanism is bound cleavage around the unsaturation of carbon chain in the β position, so a butadiene molecule is formed. Butadiene is then converted into aromatics through a Diels-Alder reaction by addition of an ethylene. In other words, the presence of unsaturation enhances the cleavage in proximity of double bonds (as α , β position of $\text{C}=\text{C}$) of fatty acids, leading to the formation of C5 to C10 alkanes.

Since vegetable and plant oils contain a complex mixture of unsaturated and saturated triglycerides, Idem et al (1996) [25] studied the thermal cracking of canola oil in the presence and absence of steam and postulated a reaction scheme to account for the thermal cracking of both the unsaturated and saturated components. A relevant issue of this model is the study on initial decomposition of triglycerides, that takes place with the cleavage of the $\text{C}-\text{O}$ bond (which generates fatty acids and acrolein as intermediates), or the $\text{C}-\text{C}$ bond in the β position (full carboxylic-group removal) leading to the formation of the $\text{C}=\text{C}$ bond into a paraffin chain, due to the absence of free Hydrogen. However, the cleavage in proximity of the $\text{C}=\text{C}$ bond of the unsaturated fatty acid chains can occur simultaneously. Another recommended reaction scheme for thermal cracking of canola oil has been shown in the following scheme, proposed by Sadrameli et al (2011) [26]: this reaction pathway tries to include more reactions to explain how a molecule of triglyceride is cracked. Authors underline that the reaction mechanism has been prepared based on the previous works and it has not been completed yet. According to this scheme triglycerides first dissociate at carboxyl group positions through reaction (1) and a precursor radical of fatty acids and acroleins are involved. They can convert to related molecules or continue to the next reaction steps. The next step is deketonization and decarboxylation of these radicals to form long chain hydrocarbon radicals through reactions (2)–(4). Reactions (5)–(7) define how hydrocarbons products are cracked and isomerized or form branched radicals, while reactions (8) and (9) describe the formation of aromatic and cyclic hydrocarbons. The last reaction (11) explains cracking of formed unsaturated fatty acids to lighter fatty acids and hydrocarbons.

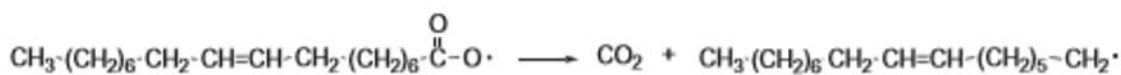
1. Thermolysis of the TG ester bond:



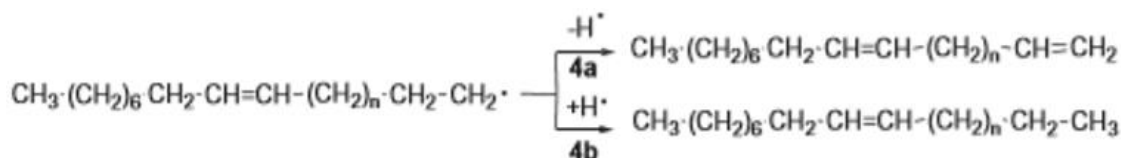
2. Deketenization (continuation of reaction 1a):



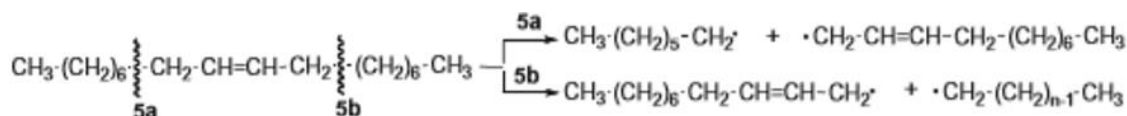
3. Decarboxylation (continuation of reaction 1b):



4. Stabilization of radicals:



5. Cracking of unsaturated HCs (shown for the predominant allyl position):



6. Isomerization:

a. Moving the double bond:



b. Forming more stable radicals:

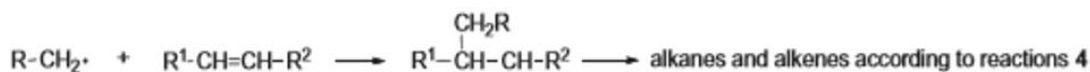


7. Formation of branched radicals:

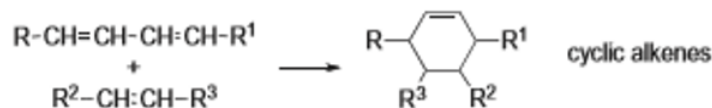
a. Direct isomerization to form more stable radicals:



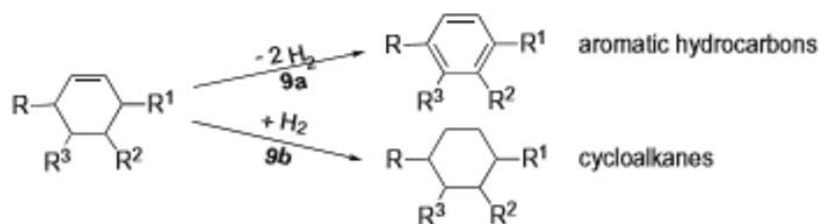
b. Reactions of radicals with double bonds:



8. Diels-Alder reaction (one of the possible pathways toward the formation of cycles):



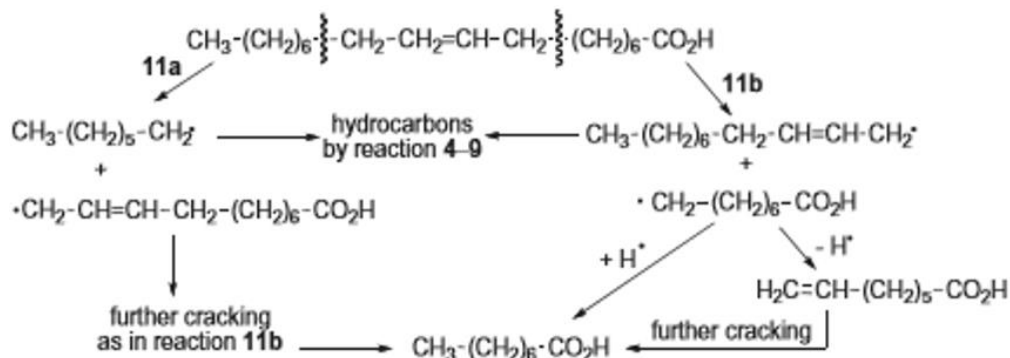
9. Hydrogen abstraction and dehydrogenation:



10. Termination:



11. Fatty acid cracking (previously unknown or uncommon reactions):



All these schemes study the reaction mechanism of triglycerides' cracking, but in case of fatty acids' cracking the reaction is slightly different: in fact, the reaction is more influenced by the saturated and unsaturated fatty acid nature. Numerous authors [19,20,27,28] report that saturated carbon chains are more stable than unsaturated ones and so there are more possibilities to remove the carboxylic group for the former. In general, the presence of unsaturation favours cracking in the proximity of C=C bonds like shown in Figure 8, but the corresponding energy level of cracking depends on their position along the carbon chain, the temperature and the catalysts type.

About fatty acids, Maher and Bressler [29] performed an experiment with stearic acid (C18:0) at different temperatures (in a range between 350 and 500 °C) and different reaction times (in a range between 0.5 and 8h) in a batch reactor. The results show that thermal cracking of the hydrocarbons occurs after decarboxylation, followed by tertiary reactions including isomerization, addition, and aromatization as the severity of the reaction conditions is increased. The following scheme (Figure 9) explains the various steps of the reaction.

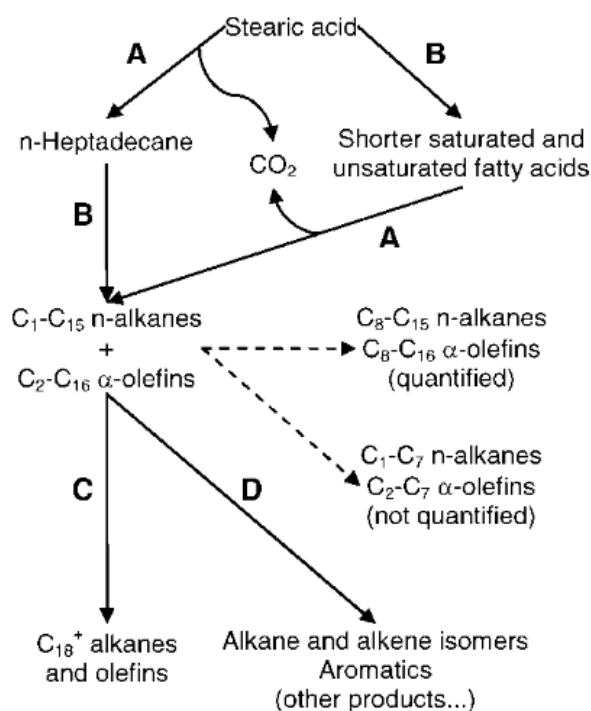


Figure 9: Thermal cracking of stearic acid by Maher et al [29].

Finally, Seifi and Sadrameli [20] reviewed the history of the models for triglycerides thermal cracking, and, based on those models, they conducted some experiments of sunflower oil thermal cracking in a continuous reactor, with a range of T between 450 and 500 °C and flowrates of 10 or 20 g/h. According to test results, the authors developed a scheme of triglycerides and fatty acids thermal cracking that shows cracking of triglycerides is started by bond cleavage at their carboxyl group positions in the liquid phase. Low temperatures increase the chance of radicals to join and/or decarboxylate. Many of the fatty acid tails of triglycerides are released as free fatty acids, some of them decarboxylated and few remain in the form of ester. Carboxyl groups, especially, in the unsaturated fatty acids are more stable than their carbon chains, so carboxyl groups are distributed among all the compounds of the organic liquid products of the process. Formation of water and CO_2 are more probable to occur in the first step of the cracking in the liquid phase. Reactions of acrolein are the same as per free fatty acids.

These studies show the complexity of pyrolysis reactions and the wide variety of products formed from the cracking of triglycerides molecules alone. Due to the lack of detailed knowledge on cracking reactions, the diverse distribution of chemical constituents generated under different conditions is only partially understood.

Non-catalytic conversion

This section investigates thermal cracking, also known as traditional pyrolysis, in which lipids are converted into smaller compounds when subjected to high temperatures in absence of catalysts. Only a few studies have been conducted on the non-catalysed pyrolysis of triglyceride or fatty acids. The reaction involves the use of an inert atmosphere often at ambient pressure. The process can be conducted either in batch, or in continuous mode, and the scale of experiments can range from reactors able to process a few grams to several kilograms of feed. Many experiments reported in this sector are resumed in Table 1. The considered parameters are reactor geometry and working condition, reaction temperature, pressure and time. All tests are done with lipid feedstock, from simple fatty acids (stearic acid, behenic acid, oleic acid, etc.) to more complex vegetable oils (soybean oil, sunflower oil, etc.) including WCO; moreover, reaction products are considered with particular attention to the hydrocarbon content. The relevant results consist in the hydrocarbon fraction collected in a liquid product, or bio-oil. While liquid yield ranges from 45 – 75 wt.% of total feed, hydrocarbons yields are usually divided by carbon classes. Among all the articles reported in Table 1, three in particular have been selected because they reported the best liquid yields.

Ling et al [1] carried out a temperature programmed pyrolysis of high acid value waste cottonseed oil (WCO) and virgin cottonseed oil in a batch type reactor. The authors have obtained a liquid yield in the 80 – 90 % range for both the WCO and for the virgin cottonseed oil (Figure 10), and it compounds mainly from methyl esters and hydrocarbons. The pyrolysis reactions were carried out respectively at different heating rates of 5, 10, 15 and 20 °C/min from 150 to 600 °C. Each reaction run, based on 5 g of WCO or virgin cottonseed oil, was carried out at heating rates repeated three times to have a tripled. Finally, using the iso-conversional method the activation energies for the pyrolysis of both feedstocks were estimated.

Heating rate (°C min ⁻¹)	Product Yield (wt.%)			
	Pyrolytic oil (W _L /W _o)	(AV) (mg KOH g ⁻¹)	Residue char (W _S /W _o)	Gas ^a (W _G /W _o)
5	81.56 ± 1.04	(166.26 ± 3.50)	6.34 ± 0.76	12.08 ± 1.65
10	83.50 ± 0.73	(163.52 ± 5.39)	4.65 ± 0.55	11.85 ± 0.62
15	85.78 ± 0.48	(155.54 ± 2.02)	3.86 ± 0.33	10.35 ± 0.77
20	86.69 ± 0.66	(147.98 ± 1.32)	3.04 ± 0.23	10.26 ± 0.90

Heating rate min ⁻¹)(°C min ⁻¹)	Product Yield (wt.%)			
	Pyrolytic oil (W _L /W _o)	(AV) (mg KOH g ⁻¹)	Residue char (W _S /W _o)	Gas (W _G /W _o)
5	87.01 ± 0.62	(152.91 ± 3.57)	2.71 ± 0.36	10.28 ± 0.72
10	89.49 ± 0.74	(144.04 ± 6.57)	1.75 ± 0.31	8.76 ± 0.62
15	89.83 ± 0.73	(138.71 ± 1.00)	1.48 ± 0.21	8.68 ± 0.55
20	90.87 ± 0.50	(133.87 ± 1.36)	1.05 ± 0.09	8.07 ± 0.51

Figure 10: Liquid yield for WCO and virgin cottonseed oil respectively [1].

Shirazi et al [30] studied the conversion of soybean oil in a continuous pyrolysis system with feed injected through an atomizer (shown in Figure 11). This allowed the introduction of micron-sized droplets of oil that are rapidly vaporized inside the reactor, so to avoid using the transport gas system. This solution could be ideal for a possible process of industrial production. At the optimum experimental conditions of 500 °C and 60 s, the yield of pyrolysis liquids was as high as 88 % (relative to feed mass). Under these conditions, the identified products consisted of 38 % hydrocarbons (22 % C₅ - C₁₂ and 16 % > C₁₂), 33 % long-chain fatty acids (C₁₆ - C₁₈, but primarily oleic acid) and 15 % short-chain fatty acids (C₆ - C₁₂).

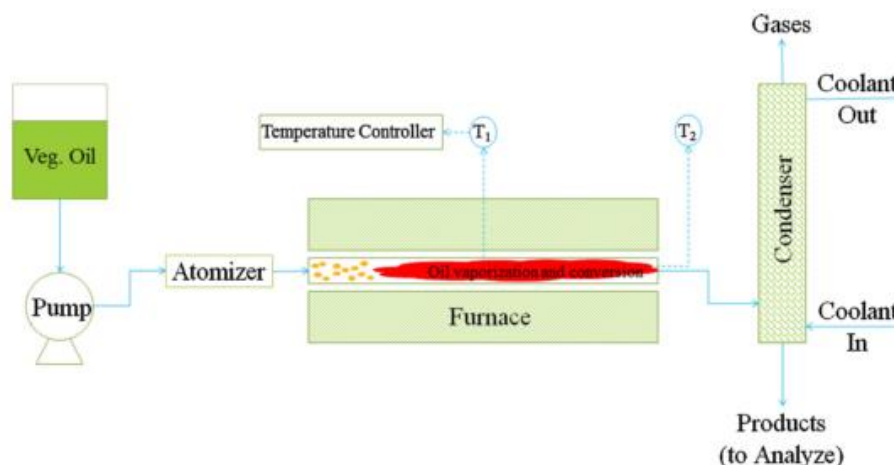


Figure 11: Schematic diagram of the pyrolysis system used by Shirazi et al [30].

Finally, Lin Xu et al [31] obtained up to 90 % of liquid yield from the pyrolysis of plant acidified oil. The numerous analysis made after tests showed that except alkane, alkene and oxygen containing compounds, plant sterol derivatives were also detected. Also, some products generated by the hydrogenation and polymerization reaction were found. The acid value and viscosity of pyrolysis products were relatively high compared to diesel oil. The calorific value had no difference with that of diesel oil.

However, almost all the articles underline that bio-oil obtained from the pyrolysis process, has to be treated to be used in the current commercial system.



Table 1: Overview on non-catalytic experiments of thermal cracking of lipid-based feedstock.

Working condition	Feedstock	Process Temperature	Reactor geometry	Atmosphere	Pressure	Feed	Residence time	Reaction time	Liquid Yield	Main Products	Notes	Reference
Batch or continuous	-	[°C]	-	-	[bar]	-	[s]	[h]	%weight	-	-	-
Batch	Oleic acid	430 - 450	15 mL batch microreactor made from 3/4 in. stainless steel Swagelok fittings, and tubing.		Not specified	1 g	-	2	70 - 80	Alkanes and alkenes (22-25%), aromatics (5-10%), cyclics (8-10%), fatty acids (4-8%).	Test made with water too.	[32]
Batch	Oleic acid	410	15 mL batch microreactors constructed with stainless steel Swagelok fittings and tubing (0.75-in.).		9 – 34.5	1 g	-	2	74 - 81	Alkanes and alkenes (C6-C19), fatty acids (C4-C18).	Constant agitation. Pyrolysis reaction in presence of short-chain alkene gases resulted in a marked increase in the liquid product yield.	[33]
Batch	Oleic acid	390 - 410	15 mL batch microreactors constructed with stainless steel Swagelok fittings and tubing (0.75-inch).		Not specified	1 g	-	4 - 8	Not specified	19.62% n-alkanes (C6-C20), 8.65% fatty acids, 10.41% internal alkenes (C6-C17), 38.64% unidentified, 2.5% 1-alkenes (C6-C17), 0.41% aromatic.	Constant agitation.	[27]
Batch	Stearic acid	350 - 500	15-mL batch microreactors constructed with 0.75-in. stainless steel tubing and Swagelok fitting.		1	0.25 - 5000 g	-	0,5 - 8	60 - 66	N-alkanes and alkenes (n-heptadecane, C7-C20), aromatics, insoluble solids, and unidentified low-molecular-weight species.	10 bar at 370 °C, 31 bar at 450 °C. More test in mild and severe conditions.	[29]
Continuous	WCO - FAs	550	Fixed bed reactor.		1	1.5 kg/h	Not specified	-	60	40% fatty acids unconverted, 13% hydrocarbons.	Tests made with catalytics too.	[19]

Continuous	WCO	800	Fixed-bed reactor (stainless steel made, 30 cm height and 15 cm internal \varnothing).		Not specified	Not specified	Not specified	-	80	Alkanes, alkenes, cyclic hydrocarbons, carboxylic acids, aldehydes, ketones, alcohols, esters, etc.	Heating rate 15 °C/min. Present 1.2% of water.	[2]
Batch	WCO	400 - 450	Batch type reactor on a mini-laboratory scale.	Not specified	Not specified	5 g	-	1	89.5	Entadecane, 9-octadecene, n-heptadecane, n-hexadecanoic acid, 9-hexadecenal, 7-tetradecenal, etc.	Heating rate of 10°C/min from RT to 600 °C. Liquid yield depends from acid values of WCO.	[1]
Batch	Oleic and palmitic acid	300 - 350	Not specified	Not specified	Not specified	40 g	-	1 - 24	Not specified	Shorter saturated fatty acids (>60%), hydrocarbons (36%), alcohols, aldehydes, esters, and ketones.	To simulate brown grease was used Fe (III) in half experiments.	[28]
Continuous	WCO - CC	550	Fixed bed reactor, 2520 stainless steel tube with an internal diameter of 51.5 mm and a freeboard height of 785 mm.		Not specified	Not specified	Not specified	-	68.6	Carboxylic acids (57.1%), aldehydes (2%), alcohol (2.68%), ketones (2.74%), phenols (3.6%), and in little amounts alkanes (6.41%), alkenes (14.8%), esters (3.51%), aromatics (4%), etc.	HHV of 32.78 MJ/kg. Heating rate of 20 °C/min. The experiments completed when no further significant release of gas was observed (approximately for 30 min).	[3]
Continuous	Soybean oil	450 - 500	Stainless steel tube with an inner diameter (ID) of 2.18 cm and length of 23 cm served as the pyrolysis reactor.		1	1 – 0,006 g/min	1 - 300	-	88	38% HCs (22% C5 - C12 and 16% > C12), 33% long-chain fatty acids (C16 - C18, but primarily oleic acid) and 15% short-chain fatty acids (C6 - C12).	A high temperature ultrasonic atomizer (4 mm of diameter) was attached to one end of the reactor tube to introduce soybean oil into the reactor.	[30]

Batch	Sunflower oil	425 - 470	Glass boat (d=15.0 mm, W=250.0 mm), inserted into a borosilicate glass reactor (d=30.0 mm, W=50.0 mm). This assembly was placed inside a tubular furnace.		Not specified	20 g	-	Not specified	78.6	F1: 22.6% acids, 54.7% hydrocarbons, 22.7% others. F2: 42.7% acids, 46.7% hydrocarbons, 10.7% others.	Sunflower oil was heated at a heating rate of 8 °C/min, remaining 10 min at 425 °C. After the remnant oil was heated to 470 °C with a heating rate of 8 °C/min.	[34]
Batch	Sesame and Mustard de-oiled cakes	350 - 700	Semi batch reactor	Not specified	Not specified	30 g	-	0.4 – 0.2	58.5 – 53.2	Octadec-9-enoic acid, indole, methylolinoleate, oleanitrile and hexadecanoic acid methylester.	Calorific values 25.5, 25.1 MJ/kg. Heating rate of 25 °C/min.	[35]
Continuous	Palm, olive, rapeseed and castor oils	750	CDS Pyroprobe 1000 heated-filament pyrolyser.	Not specified	Not specified	700 – 900 µg	20	-	Not specified	Linear monoalkenes (up to C19) and alkanes (up to C17). Positions appeared as well. The volatile products marked as “C3–C6 compounds” primarily corresponded to both alkenes and alkanes.	Heating rate of 1000 °C/s. Hydrolysis of palm, olive and rapeseed oils mainly resulted in volatile products.	[36]
Batch	Plant acidified oil	500	Vertical stainless steel, which was a batch reactor (length: 600 mm; inner diameter: 38 mm).		Not specified	Not specified	-	2	90.1	The peak area of alkene, fatty acid, alkane and alcohol was about 41.57%, 32.5%, 9.51% and 3.11%, respectively. About 5.88% plant sterol pyrolysis derivative was also found.	Heating rate of 10 °C/min. The calorific value has no difference with that of diesel oil. The acid value and viscosity of pyrolysis products were relative high compared with diesel.	[31]

Batch	Soybean oil	380 - 400	The SC, a 46-cm straight condenser and a thermocouple are coupled to a two-mouthed round-bottomed flask which serves as the reactor. The MC uses of a 25-cm straight condenser without the passage of water which is coupled to a flask. In the FC the straight condenser of is replaced by a 31-cm-long Vigreux column.	Not specified	1	200 g	-	2.5 (SC) – 4 (MC) – 5.33 (FC)	84 (SC) – 63 (MC) – 47 (FC)	Oxygenated compounds such as alkanes, alkenes, aromatics, carboxylic acids, ketones and alcohols were identified. The HCs present in the light fraction are C4–C14, and C2–C8 oxygenated compounds. The heavy fractions presented C6–C30 linear HCs, with C8–C20 oxygenated compounds.	The experiments were carried out using three different systems: simple cracking (SC), modified simple cracking (MC) and fractionated cracking (FC). These tests execute also with catalyst.	[22]
Continuous	Sunflower oil	450 - 500	A quartz tube with the dimension of 20 mm × 650 mm × 1.5 mm (OD × L × thk.) was used as the bed reactor that was placed vertically and centered in the furnace.		1	10 – 20 g/h	Not specified	-	66.6 – 89.9	Not specified	Liquid yield is better for flowrate higher. These experiments are focused on the study of thermal cracking, no on the optimization of pyrolysis process.	[20]
Batch	Linoleic acid	350 - 450	Stainless steel Swagelok fittings and tubing (0.75 in.) and heated in a fluidized bed sand bath (Techne, Burlington, NJ).		Not specified	1 g	-	0.5 - 8	71.1 – 86.3	The major products at low T and t are C7, C10, C7:0, C8:0, n-heptadecane and octadecanoic acid. As high T and t a reduction in FAs, 1-alkenes, internal alkenes and an increase of cyclic and aromatic compounds	The microreactor was heated at the desired temperature under constant agitation.	[37]
Batch	FAs	410	Stirred 1 L reactor (Parr Instrument Co., Moline IL) heated by an electric heating element located outside of reactor.		1	100 g	-	1.5	76 - 80	Predominantly of n-alkanes (C6 – C23).	A stirrer are used at 300 rpm.	[38]

Continuo us	Canola oil	300 - 500	Stainless steel (SS-316) with 10 mm i.d. and 508 mm overall length heated by a furnace with T controlled by a series of SR22 PID temperature controllers using a K-type thermocouple.		1	5.1 – 24.2 g/h	Not specified	-	14.4 – 45.9	The main chemical groups included light paraffin gases, C2–C4 olefins, C4–C5 gases, alcohols, ketons, aldehydes, aromatics and coke.	The residence time of the reactor is controlled by the flowrate and length of the reactor.	[39]
Continuo us	WCO	475 - 525	Pilot plant for thermal cracking operating in a continuous mode under isothermal conditions.	Not specified	1	0.75 - 3.65 kg/h	15 - 80 s	-	40 – 80 (C4-C11); 25 – 30 (C12-C18); 5 – 40 (>C18)	WCO (>C18), heavy bio-oil (C12-C18), light bio-oil (C4-C11) and and bio-gas (<C4).	The article analyses like results only WCO (>C18), heavy bio-oil (C12-C18), light bio-oil (C4-C11) and and bio-gas (<C4).	[40]
Continuo us	Canola oil	450 - 580	The pilot plant is constructed as a reaction/regeneration system with an internal circulating fluidized bed system. Both reactors (riser, regenerator) are built in one apparatus		1	2.5 kg/h	20 – 80 s	-	87.4 (480 °C)	Gasoline is 21.1 wt% at 450 °C and 34.5 wt% at 580 °C. It consists mainly of saturated HCs, than olefins and aromatics.	High total fuel yields (>77 wt%) is achieved at all temperatures (77.2 % at 450 °C and 84.9 % at 580 °C).	[41]
Batch	Jatropha oil	300 - 375	Not specified		1	5 g	-	2 – 10 min	73	The liquid product obtained to contain alkanes, alkenes, cycloalkanes and carboxylic acids.	The experiments were carried out at different heating rates of 5, 10, 15 and 20 K/min. The flow of nitrogen was maintained at 120 ml/h for the course of the reaction.	[42]

Catalytic conversion

While the production of biodiesel is commonly based on the use of liquid catalysts, the catalytic conversion (that generally consists in catalytic pyrolysis processes) adopts solid catalysts. Generally, the use of solid acids and bases induces several benefits such as: easy separation and recycling. Solid acids are safer and easier to handle than their liquid counterparts, indeed, contamination of the product by trace amounts of (neutralized) catalyst is generally avoided when the latter is a solid. Therefore, in the recent past, various metal catalysts, such as Pd-, Pt-, and Ni-based catalysts, have been applied for deoxygenation reactions; among them, Pd-based catalysts exhibit the best catalytic activity in deoxygenation reactions [43]. However, noble metal-based catalysts could significantly raise the cost of deoxygenation processing: in fact, for hydrotreating processes these expensive catalysts limit their diffusion [11]. The deoxygenation reaction does not need a catalyst to occur, but catalysts enable a pyrolysis reaction in less severe conditions. In particular, for catalytic pyrolysis noble metal-based catalysts are not required, so in recent years many less expensive catalysts have been developed [11,15,43,44].

A comprehensive list on the variety of adopted catalysts in a catalytic conversion of vegetable oils was investigated by Idem et al [45], and reported in Figure 12. Major groups of catalysts used in catalytic thermal cracking processes include molecular sieve type catalysts (i.e. zeolites), metal oxide catalysts (both basic and acid sides) and some others not included in these categories.

Catalyst	Characteristics							
	Acidic, basic or neutral	Type of acidity	Si/Al ratio	Strength of acid or basic sites	Pore structure	Pore size. (nm)	Surface area (m ² g ⁻¹)	Shape selectivity
HZSM-5	Acidic	Mostly B	56	Strong (acid)	Uniform and crystalline	0.54	329	Very high
Silicalite	Neutral	None	No Al	N/A	Uniform and crystalline	0.54	401	Very high
Silica	Neutral	None	No Al	N/A	Amorphous	11.46	211	None
γ -Alumina	Acidic	B and L	0	Moderate (acid)	Amorphous	14.93	241	None
Silica-alumina	Acidic	B and L	0.79	Moderate (acid)	Amorphous	3.15	321	None
Calcium oxide	Basic	None	N/A	Strong (base)	Amorphous	11.86	7	None
Magnesium oxide	Basic	None	N/A	Weak (base)	Amorphous	15.22	27	None
Empty reactor	Neutral	None	N/A	N/A	N/A	N/A	None	None

Figure 12: Catalysts list by Idem et al [45].

Chemical energy assessment

This section aims to report the literature research as well as chemistry data about bond breaking in fatty acids and triglycerides: in fact, the scope of this work is to study the C-O and C-C bond cleavage, so that in a thermal cracking process it will be possible to remove an oxygen atom from the carboxylic group of fatty acids. Therefore, this process can generate liquid rich in hydrocarbons and can considerably ease possible and subsequent treatment to obtain pure hydrocarbons. For example, in the previous chapter the HVO process is reported and explained: it is a promising process but the high necessity for hydrogen in high pressure limits its diffusion. Thus, if a pre-treatment can be found to make a less expensive and less complicated HVO process, it has to be elaborated. The removal of oxygen atoms from triglyceride or fatty acids is necessary because the presence of oxygen lowers the heating

values of biofuels, which are lower than those of conventional fuels on a mass basis, and can also cause stability problems [4].

The energy needed to break molecular bonds is reported in Table 2 that demonstrates the binding energies (BE) of the bonds present in a triglyceride in kJ mol⁻¹ found in different references.

Table 2: Binding energies values present in different sources.

C-O	C-C	C-H	C=C	O-H	C=O	Reference
335	347	414	619	678	707	[46]
-	348	412	612	463	743	[47]
352	348	-	-	463	-	[48]
360	350	410	611	464	740	[49]
-	368	410	720	463	725	[50]
-	347	414	522	469	-	[51]

Among the bonds present in a triglyceride, the C-O and C-C bonds are the ones with the lowest BE, and this can suggest that their cleavage occurs in non-critical conditions, like low temperatures and low heating rates. Chiaramonti et al [19] reported that the cleavage of the C-O bond takes place at the temperature of about 288 °C while the C-C bond in the β position occurs at about 388-426 °C. However, the initial pyrolysis (at a temperature above 400 °C) may begin with the simultaneous cleavage of C-O bonds and double carbon bonds (C=C) in the β position. Of course, the bonds breakage doesn't just depend on the BE, but another very important parameter is the presence of unsaturated fatty acids: numerous authors [19,20,27,28,37,52,53] reported that the presence of a double bond in the hydrocarbon chain weakens the adjacent C-C bonds and increases the possibility that the first breakage occurs in these points, or in any case it occurs at the same time of other breakages. Many other conditions influence the cracking of the triglyceride and fatty acids and many are still not fully understood.

As shown in the last paragraph, many authors tried to explain the thermal cracking reaction mechanism in triglycerides and fatty acids and the C-O and C-C bonds breakage is one of the main points of their analysis. Seifi and Sadrameli [20] executed a very deep analysis about this topic: they carried out a pyrolysis test in a continuous reactor at T=450-500 °C and atmospheric pressure, using sunflower oil as feed. Based on their results, they reported in Figure 13 the percentage of the removed carboxyl group:

No.	Temp. (°C)	Flow Rate (g/h)	Total Carboxyl Groups Content (mg KOH/g)			Removed Carboxyl Groups (%)	
			Organic Liquid Product	Cuts			
				10-150 °C	150-250 °C		250-350 °C
1	500	20	129.34	119.89	153.79	140.28	29.6
2	500	10	96.42	80.47	99.31	103.87	47.5
3	450	20	134.90	98.68	145.69	103.20	26.6
4	450	10	77.06	81.18	80.38	68.80	58.1

Figure 13: Total carboxyl group remained in bio-oil of the cracking products [20].

While the total carboxyl group of the feed was 183.73 mg KOH/g, the amount of carboxyl groups which have remained in the bio-oil after testing, show that some of them have been converted but a large amount of the groups have remained in the liquid form. Figure 13 also shows the almost smooth distribution of carboxyl groups in different cuts of bio-oil: this means that the carboxyl groups have fewer tendencies to crack than carbon chains in the fatty acid tails of triglycerides and therefore are more stable. Then based on the reaction conditions, 26.6–58.1 % of carboxyl groups in feed will disappear in the form of water, CO₂ and other compounds. In the following Figure 14, the authors report also the most probable triglyceride reaction cracking based on their studies:

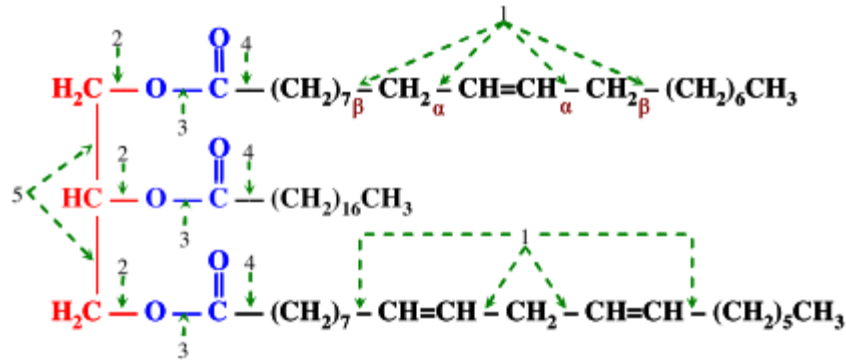


Figure 14: More probable bound cleavage during thermal cracking of triglyceride [20].

One condition much reported in literature [19,22,26,30,34] is that the most likely first bond breakage of a triglyceride is represented by the C-O bond breakage in position 2; Seifi and Sadrameli confirm this solution given the high acidity of products that suggests the free fatty acids formation from the triglyceride molecule. As the results show, some carboxyl groups in the ester form are found in all cuts and so two cases can be considered: breaking at point 5 or cracking at point 1 before others. The production of light cuts shows that some bound cleavages take place along the carbon chain of fatty acids. If the carbon chain is unsaturated, the breakage in the α or β position relative to the double bond is more probable (at breaking point 1). The reduction of the carboxyl group evidenced in Figure 13, shows some bond cleavage takes place in points 3 or 4 and the carboxyl group releases CO_2 and H_2O . This is the decarboxylation reaction, but it is less probable compared to the C-O bond cleavage among the glycerol and fatty acids molecule: in fact, the authors conclude that, considering their data, 2/3 of the bound cleavage takes place at point 2, while 1/3 at point 3.

Sadrameli et al [26], as presented previously, review the experiments made with vegetable oils in a temperature range of 300-360 °C and atmospheric pressure, without a catalyst.

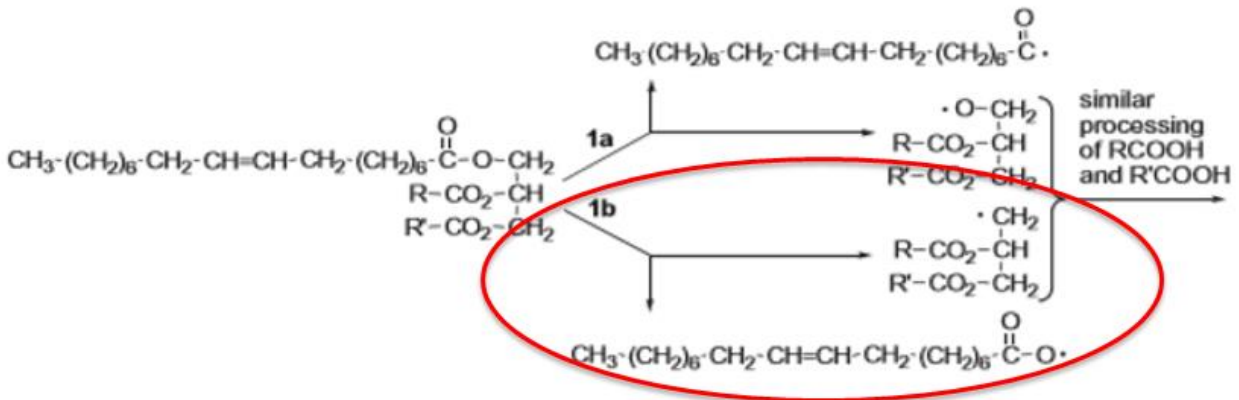


Figure 15: Extrapolation of the first bond cleavage from reaction mechanism by Sadrameli et al [26].

Figure 15 shows the most likely first bond breakage of a triglyceride. The authors, considering their data, assert that at low temperatures, the decarboxylation is blocked and therefore reaction progresses following reaction 1b and forming mostly molecules of long free fatty acids. They also show kinetic experiments in which triglyceride ester bonds completely break down within a few minutes or even seconds at temperatures higher than 350 °C.

Maher and Bressler [29] instead study stearic acid (C18:0) thermal cracking. The fatty acids reaction is more complex compared to the triglycerides thermal cracking: comparing the numerous articles it is possible to notice that on average, triglycerides cracking starts at lower temperatures compared to fatty acids. This is probably due to the greater ease of breakage of the C-O bond between glycerol and fatty acid molecules and the subsequent radical formation. As already mentioned, the fatty acids cracking depends mostly on the saturated or unsaturated molecule nature: saturated carbon chains are more stable than unsaturated ones and therefore there is lower probability of breakage of a C-C bond along the hydrocarbon chain. Maher et al make thermal cracking of stearic acid in a batch reactor between $T=350-$

500 °C in environment pressure. According to their results, at the mildest conditions (low temperature, low time), very little reaction product was formed. After 4 hours of reaction time at 350 °C, n-heptadecane (C17) is the only n-alkane produced in significant quantities as shown in Figure 16: it shows the molar yields of C8-C20 n-alkanes as a function of temperature with 4 hours reaction time; solid circles correspond at 350 °C, open triangles 390 °C, solid squares 430 °C, open diamonds 450 °C (the bullet points are the average, and error bars represent the maximum).

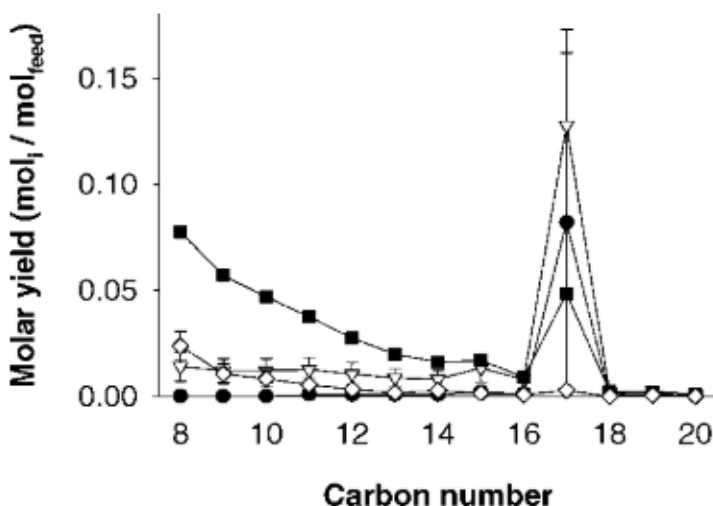


Figure 16: Molar yields of C8-C20 n-alkanes as a function of temperature for 4 hours reaction time [29].

The generation of n-heptadecane suggests that decarboxylation already occurs at $T=350$ °C. That means that it is the one significant reaction at that temperature and that the presence of oxygen (electron withdrawing atoms) in the carboxyl group weakens the C-C bond adjacent to the carboxyl group. Therefore, initiation was likely to involve homolytic cleavage of this C-C bond [27]. Once the temperature increases, the C17 amount increases to a maximum of $T=390$ °C, subsequently the n-heptadecane percentage quickly decreases.

Asomaning et al [27] executed numerous pyrolysis experiments with oleic acid (C18:1) in a range of $T=350-450$ °C and atmospheric pressure. Oleic acid is an unsaturated fatty acid, in fact the authors' results evidence some difference compared to Maher's experiments.

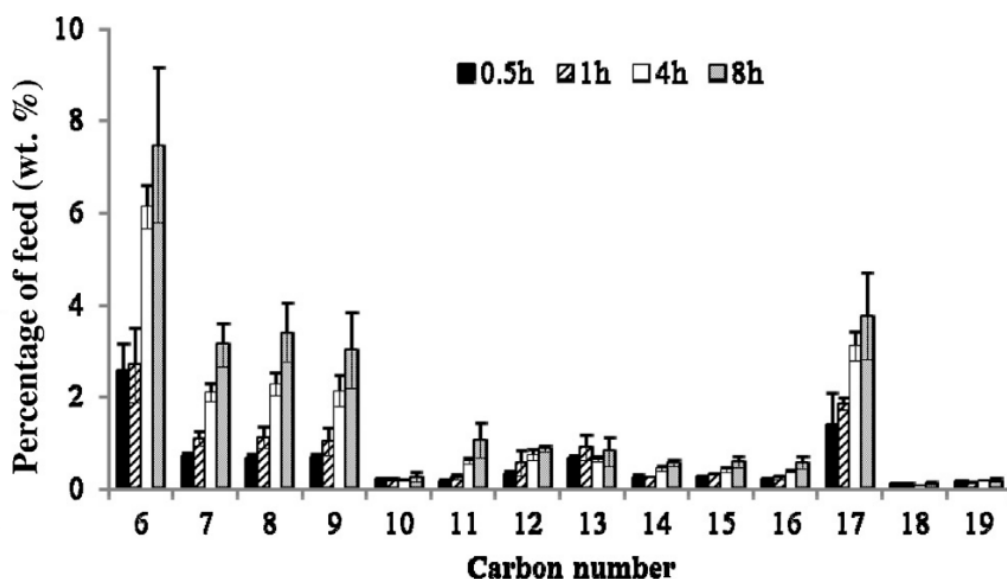


Figure 17: Percentage of n-alkanes at 390 °C as a function of carbon number and reaction time [27].

Figure 17 illustrates the main products of n-alkanes at $T=390$ °C in function of reaction time: it is soon evident that with the time increase the reaction is more complete and so a higher

percentage of feed is able to react. Confronting this graph with Figure 16 (open triangles in figure correspond at T=390 °C) it is evident that there is a larger number of hydrocarbons with a carbon number that range from C6 and C9, and simultaneously a C17 is present in significant amounts. The higher content of alkanes between C6-C9 is likely due to the presence of a double bond in oleic acid, which is the cause of the impairment and breakage of adjacent C-C bonds. Also, Omidghane et al [32] carry out the same tests using oleic acid, in an atmospheric pressure in a batch reactor and with a temperature range of 390-450 °C, and obtain similar results. Also, Sadrameli et al [26] report, in case of triglyceride and fatty acids thermal cracking, at low temperatures and long reaction times, the main products will be heavy hydrocarbons (>C14).

Both Asomaning et al and Omidghane et al in the articles mentioned above, account that at low temperatures (in a range between 350 °C and about 430 °C) the gas products contain more CO than CO₂, and this suggests that the reaction runs following mostly the decarbonylation mechanism and in a minor way the decarboxylation mechanism. This is already suggested by Sadrameli et al when they report the arrest of the decarboxylation reaction at a temperature near 350 °C.

Y. Sim et al [28] in their work make a thermal cracking of palmitic and oleic acid to simulate the brown grease pyrolysis process. They executed these processes at, 325 and 350 °C changing the reaction time (reactor type, environment pressure and atmosphere are not specified). They resumed the percentage of non-reacted starting material as a function of time and temperature in Table 3.

Table 3: Percentage of starting material remaining as a function of time and temperature [28].

Compound	T [°C]	3 h	6 h	10 h	24 h
Palmitic acid	300	>99%	>99%	98%	97%
Palmitic acid	325	97%	95%	93%	83%
Palmitic acid	350	36%	32%	18%	<5%
Oleic acid	300	79%	82%	62%	51%
Oleic acid	325	36%	6%	<5%	<5%
Oleic acid	350	<5%	<5%	<5%	<5%

The first evidenced detail is the higher reactivity of oleic acid compared to palmitic acid, due to the presence of the double bond in the first one. Palmitic acid practically does not react at 300 °C for all reaction times considered, and also at 325 °C only after 24 hours is it possible to notice the start of a relevant cracking. Only at 350 °C for 24 hours can the palmitic acid thermal cracking be considered complete. Oleic acid, due to the presence of a double bond, is more reactive and already at 300 °C presents significant thermal cracking levels. At 325 °C, the reaction is close to completeness after 6 hours, while at 350 °C it is complete for all reaction times considered. The authors also carried out a pyrolysis test with a palmitic and oleic acid mix (both at 50 %), and according to results the mix increases the tendency to react compared to single fatty acids. Thus, the lower temperature reactions of oleic acid must enhance the reactivity of palmitic acid. For example, a radical formed from thermal degradation of an unsaturated acid might extract a Hydrogen atom from the saturated acid, enabling decarboxylation and generating another radical. Finally, the authors propose a reaction sequence of palmitic acid presented in Figure 18: the ketene is reversibly formed by loss of water from palmitic acid, where it reacts with a second acid molecule to form palmitone (palmitic acid ketone) with the loss of CO₂. Even at 350 °C, minimal CO formation is observed in the author's data. Hydrocarbons are formed, possibly by decarboxylation and minimal decarbonylation, but with the ketone as the major product.

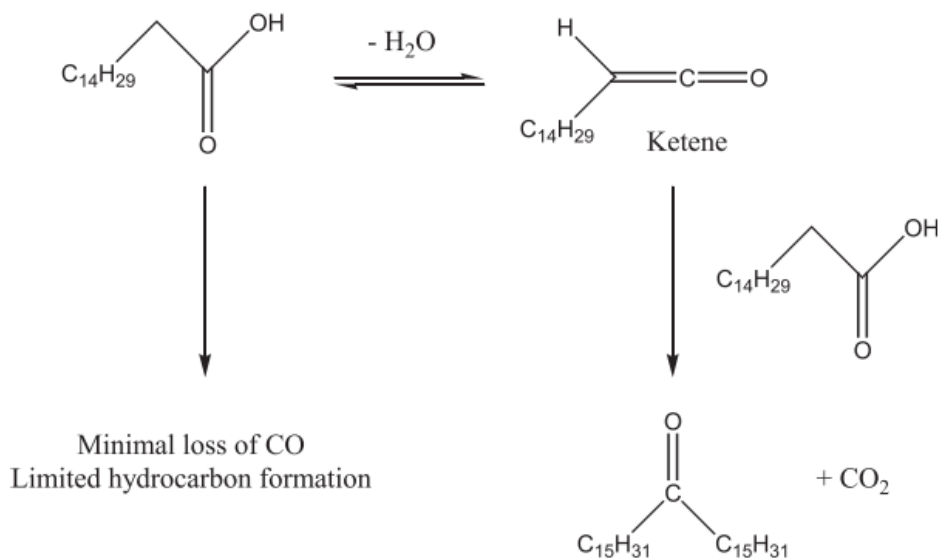


Figure 18: Proposed reaction pathways for palmitic acid [28].

Biswas and Sharma [42] choose jatropha oil (JO) to make a pyrolysis experiment in a batch reactor at temperatures of 300, 350 and 375 °C in atmospheric pressure, with different heating rates (5, 10, 15 and 20 °C/min) and low reaction times (2-10 minutes). The thermogravimetric analysis (TG) and DTG curves for thermal degradation of JO at different heating rates are shown in Figure 19. The degradation of JO is found to occur in three steps. The TG curves shows that there is a slight mass loss occurring from ambient to about 220 °C, which is due to the loss of the water present in the JO, therefore this zone signifies the drying of JO. The second step of degradation takes place from 230 to 350 °C, while the main devolatilization of the material occurs in the third zone between 350 and 480 °C and the degradation is essentially complete in this zone. The DTG curve also shows that there are two peaks observed. The first peak would be due to the breakdown of the big triglyceride molecule into smaller organic molecules, and it corresponds to temperatures near 300 °C. The second peak corresponds to the total devolatilization of the organic molecules. The authors specify that at 300 °C the JO thermal cracking is not very significant and unreacted JO oil is left behind even when reaction time is increased from 2 to 10 minutes, while the results of thermal cracking of JO at 375 °C indicate that there is a complete conversion of the JO to liquid, gaseous products and char.

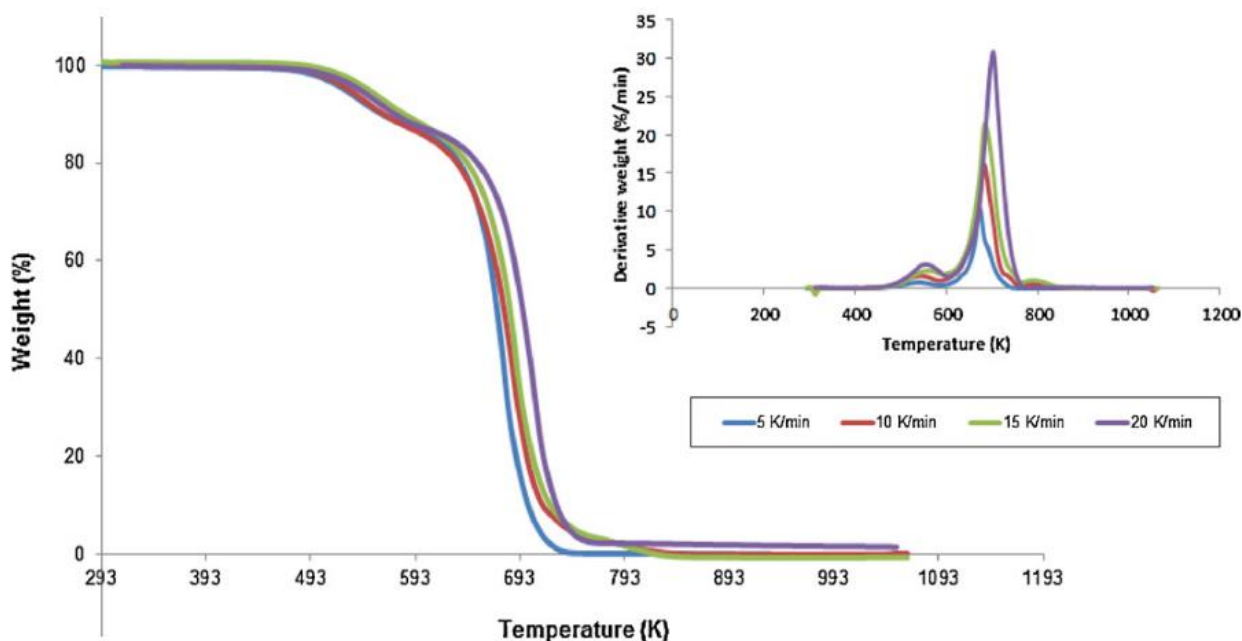


Figure 19: TG curves of JO at different heating rates. Inset corresponding DTG curves [42].

Instead Prado and Filho [22] carry out a pyrolysis experiment using soybean oil as a feedstock. It is made in three different reactors: simple cracking (SC), modified simple cracking (MC) and fractionated cracking (FC). Thermal cracking tests are carried out in a temperature range between 380 and 400 °C in atmospheric pressure and analysing the results, the authors affirm that at a temperature above 300 °C a new thermal cracking reaction starts, leading to the decomposition of long-chain fatty acids.

Another test performed using vegetable oil is made by Sadrameli and Green [39]. The authors execute a canola oil thermal cracking at temperatures between 300 and 500 °C in atmospheric pressure with a continuous reactor (residence time is not specified). In Table 4 below, the results of their tests are reported here below.

Table 4: Yields (wt.%) of the products canola oil thermal cracking as a function of temperature [39].

Mass Balance	300°C	370°C	400°C	450°C	500°C
Gas	15.0	38.0	55.8	71.7	75.0
Liquid	38.1	45.9	34.4	17.2	14.8
Coke	0	3.9	3.9	3.9	3.9
Residual Oil	41.9	6.1	1.6	1.2	0
Unaccounted	5.0	6.1	4.3	6.0	6.3

At low temperatures the residual oil is a considerable part of the product, particularly at 300 °C where it corresponds to 41.9 wt.%. Comparing the results of vegetable oils thermal cracking with fatty acids thermal cracking it is possible to observe that triglyceride cracking is on average easier at low temperatures compared to fatty acids cracking, as already mentioned above.

Commercial applications and aim of the study

Today only a Canadian company, Forge Hydrocarbons Corp. [54], is proposing the direct non-catalytic conversion of lipids (once already pre-converted as fatty acids) at commercial level. However, the most challenging outcome is to maintain high liquid conversion yield vs the produced hydrocarbons fraction into the liquid product. Even if only partial feedstock is converted, a next hydrotreatment could convert the residual non-converted fatty acids, significantly reducing the hydrogen demand. Thus, the present study aims to assess the real conversion yield of hydrocarbons and the residual non-converted fatty acids into the liquid product in order to assess the economic feasibility of this conversion pathway.

4. R&D initial work and equipment

At the beginning of the project, RE-CORD performed preliminary tests in its catalytic pyrolysis unit to investigate the effect of thermal cracking on waste lipids. Batches of used cooking oil collected from industries have been collected and analyzed (methods and results of the analysis are reported in the next section). Results of catalytic pyrolysis confirmed the results already reported in recent experimental studies of the authors (i.e. Chiaramonti et al [19]), where it has been demonstrated that the direct cracking of triglycerides is challenging since the de-oxygenation reactions happens later than generic thermal cracking reactions along fatty acids molecules (as investigated in the previous chapter). Using pure triglycerides, the target cracking reaction does not coincide with deoxygenation reaction, thus a preliminary fatty acids distillation through hydrolysis is required. Operating with pure fatty acids (in particular with saturated ones as first, to avoid other potential cracking reaction along the C=C bonds), the target conversion pathway is more probable as demonstrated by several authors in literature (see previous chapter). Thus, the most promising pathway is the use of pure stearic acid, the main constituent of used cooking oil. Thus, before doing a step back at lab scale to show and elaborate the new proposed R&D pathway (see next chapter), here following the available

demo-units at RE-CORD are presented. Demo-units will be used in a second part of the project if laboratory tests will confirm more promising results at small scale.

4.1 Catalytic pyrolysis unit

The continuous catalytic conversion unit, available at RE-CORD/University of Florence, can process 1.5 kg h^{-1} of liquid feedstock. The experimental rig is composed by a first pyrolysis fixed bed reactor, able to convert the lipids into pyrolysis vapours, that are subsequently upgraded by a second fixed-bed catalytic reactor, and finally condensed into a bio-oil (pyrolysis oil). The feeding system consists in a pressurized injection system, which pumps the feedstock into a nozzle placed in the reactor. Before the injection, the oil is heated through electrical resistors to reduce the oil viscosity and improve feedstock atomization. The pyrolysis chamber is heated up to $550 \text{ }^\circ\text{C}$, and during operation, a nitrogen flow maintains an inert environment. In parallel, nitrogen flow generates a slight overpressure that pushes the pyrolysis vapours to the catalytic reactor. The latter is properly heated by a dedicated resistor up to $550 \text{ }^\circ\text{C}$, allows catalytic upgrading of pyrolysis vapours. The condensation system consists of two watercooled condensers (water temperature equal to $15\text{-}20 \text{ }^\circ\text{C}$) connected in series, which collect the liquid product in the same point by gravity (into a LDPE bottle), and a water bubbler to remove the aerosol from non-condensable gases. Pyrolysis oil from the two condensers is collected (as mixed product) in a bottle placed at the bottom of the two condensers. Permanent gases are sucked through the whole plant by a blower and discharged. The water bubbler temperature is kept at $15\text{-}20 \text{ }^\circ\text{C}$. A picture representing the experimental apparatus is given in Figure 20.

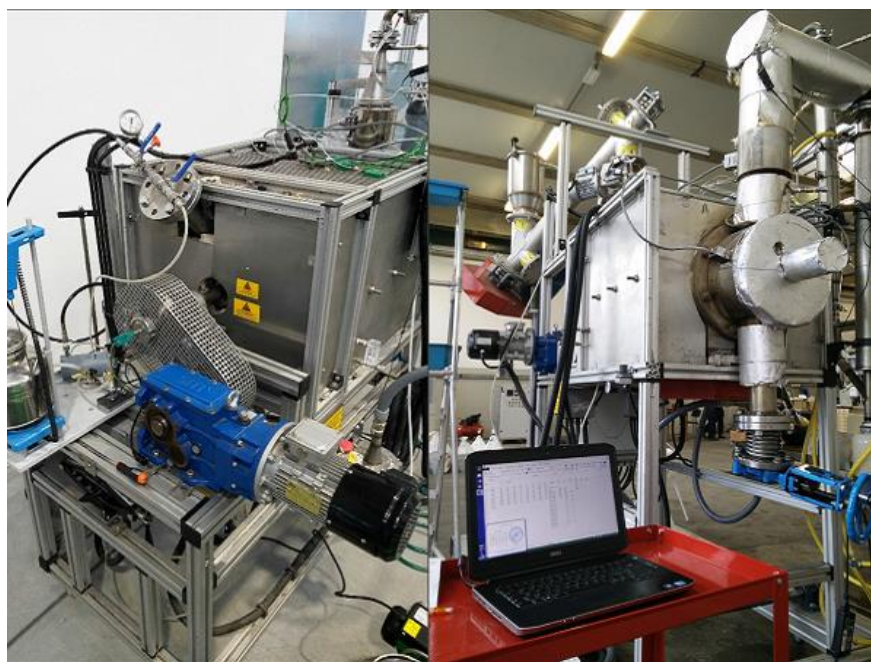


Figure 20: Catalytic pyrolysis unit at RE-CORD facilities.

The unit is currently available for lipid-based feedstock processing.

4.2 Hydrothermal liquefaction unit

RE-CORD has recently developed a continuous hydrothermal liquefaction unit, where the results from batch experiments of this thermochemical conversion process of biomass at lab scale can be validated in a continuous system. The continuous plant can elaborate more than 1.5 l/h of feedstock (generally a slurry of biomass-in-water solution). The unit is equipped with a high-pressure positive displacement pump and two different depressurization/cooling systems, which are adopted alternatively. A picture of the unit is reported here below.



Figure 21: Continuous hydrothermal liquefaction unit at RE-CORD facilities.

5. Experimental campaign: materials and methods

As briefly reported in the last chapter, RE-CORD performed a lot of efforts in the R&D pre-processing of lipids. The experience collected in last years suggested that the most promising pre-treatment process of waste lipids (such as UCO) before HVO processing, is the direct thermochemical conversion in a pressurized environment without the using catalysts. This process aims the targets of Bio4A since it does not require hydrogen and maintains low operating costs compared to pyrolysis and HTL. In the next paragraph 5.3.4, materials and methods adopted for the proposed R&D campaign of T2.3, are presented.

5.1 Feedstock and methods of analysis

UCO was supplied by SILO SpA (Florence, Italy): this company acquires raw UCO from restaurants and eating-places in the metropolitan area of Florence: the liquid is then stored in dedicated stainless steel tanks at SILO premises. Collecting samples from these UCO tanks requires the use of a special tool, named “sonda Marsigliese”, which is accepted as sampling methods for UCO batches. This instrument allows taking UCO samples at the same time from different heights in the tanks, so to ensure that the collected liquid is representative of the whole liquid stored in the tank. According to T2.3 targets, 3 batches of UCO of different origins were sampled.

Before using pure UCO, preliminary hydrolysis test have been performed with glycerol trioleate (produced by Sigma-Aldrich), pure at 65%.

The feedstock used for batch scale tests of deoxygenation is pure stearic acid (C18:0). In the third chapter, the advantages of using saturated fatty acids were explained, in particular the absence of a double bond to allow an easier separation of the carboxylic group from the hydrocarbon chain. The stearic acid was supplied by EMD Millipore Corporation with 97 % purity (Figure 22).

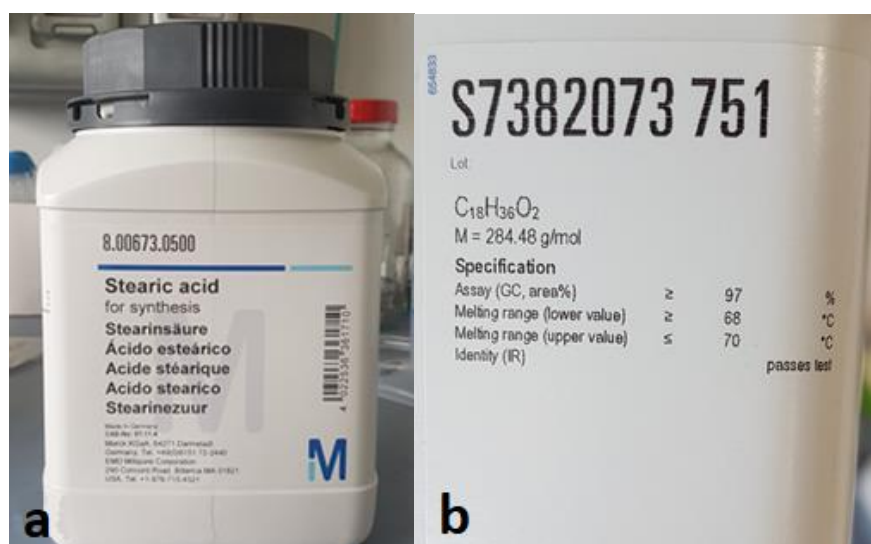


Figure 22: a) EMD Millipore stearic acid; b) Specifics of stearic acid.

These materials (i.e. UCOs, TAGs, FAs) were characterized before being used for tests according to the following procedures.

1.i. Elemental analysis

The elemental analysis was performed by LECO-TrueSpec [55]. A 50-100 mg sample was used to perform the determination of C, H, N, while oxygen content was obtained by difference. The TruSpec Add-On Module was used for the determination of Sulphur

content according to an internal method. As regards nitrogen content, in order to achieve a higher sensitivity than LECO-TrueSpec, a Thermo Finnigan FlashEA 1112 NC analyzer [56] was used.

i. LHV and HHV determination

HHV was determined by a LECO-AC500 calorimeter [57]. LHV was calculated from HHV taking into account moisture and Hydrogen contents [58].

ii. Acid value and free fatty acid content

The acid value, used to assess the free fatty acid concentration in the UCO, was evaluated as the amount (milligrams) of potassium hydroxide necessary to neutralize a mixture of the sample blended with a proper solvent (ethanol: diethyl ether, 1:1 volume ratio). A manual titration is used as reference method for this analysis [59]. A more detailed description of titration method used for cracked products analysis is reported in paragraph 5.3.4. The determination of free fatty acid content was verified [60], halved than acid value for vegetable oils. The acid value is expressed as a mass fraction; the free fatty acid content is expressed as a percentage mass fraction.

iii. Kinematic Viscosity

Kinematic viscosity of feedstock and pyrolysis oil was determined at 40 °C by a LAUDA Proline PV15 viscometer [61].

iv. Water content

The water content was measured by Karl Fisher's titration [62] for feedstock. For the pyrolysis products, the water content is determined with the modified procedure proposed by Oasmaa and Peacocke [63].

v. Total contamination

Total contamination was measured by a high retention glass-fibre filter of 0.7 µm (mean pore size), solubilizing the sample in n-heptane [64].

vi. Density

Density of liquids was measured at 15°C by a calibrated glass hydrometer [65].

vii. Ash

Ash was determined with a Leco TGA 701 by heating up to 750 °C and holding there for at least 1h 30min [66].

viii. Chemical class composition by gas chromatography techniques

The composition of hydrocarbons, fatty acids and other compounds in the pyrolysis oils was measured using GC-MS (GC 2010 with a GCMS-QP2010 mass spectrometer, Shimadzu) and GC-FID (GC 2010 Plus-Shimadzu). Both analyses were performed using 500 mg of sample, dissolved in 25 cm³ of isopropanol and then injected (1 mm³) in split mode; the used column was a Zebron ZB-5HT INFERNO (Phenomenex) (length 30 m, internal diameter 0.250 mm, film diameter 0.25 µm). The analysis was performed with a column flow of 2.02 cm³ min⁻¹ for GC- MS and 3.17 cm³ min⁻¹ in GC- FID with an initial temperature of 40 °C (holding time 10 min) increased to 200 °C (heating rate 8 K min⁻¹, holding time 10 min) and then to 280 °C (heating rate 10 K min⁻¹, holding time 30 min). For GC-MS the mass to charge ratio (m/z) ranged from 35 to 350. Compounds were first identified in GC-MS by the comparison of their mass spectra with the NIST library. For quantification of specific chemical compounds in GC-FID, their response factors, relative to the internal standards o-terphenyl or D-6 benzene, were determined by using standard compounds injected in a range of concentrations that reflects those found in the samples. All standards are provided by Sigma Aldrich. Regarding the hydrocarbons standards the compound considered were n-paraffins, n-olefins, aromatics (BTEX and PAHs), As chromatograms of catalytic intermediate pyrolysis of lipid-based materials show a hump at

the central zone (at about 15-30 min), similar to diesel/gasoline chromatograms, even if less accentuated, in order to maintain a conservative approach as regards quantitative assessments of hydrocarbons in the pyrolysis oil mixture, a “valley-to-valley” integration has been performed, thus not considering the bottom area. This approach, while probably underestimating the actual amount of hydrocarbons, avoids possible interferences of unidentified chemicals with the pure peaks in the chromatogram and therefore overestimation of results.

5.2 Experimental apparatus

All experimental tests were carried out in MRTB or Micro Reactor Test-Bench (Figure 23). The unit is a batch reactor, containing an air-fluidized sand bed (FSB-4 Omega Engineering). The sand is heated by 4 resistors: they can make the sand reach a maximum temperature of 540 °C. Each resistor absorbs 1 kW of power, for a maximum of 4 kW when all resistors are turned on. The entire system has a voltage of 240 V.

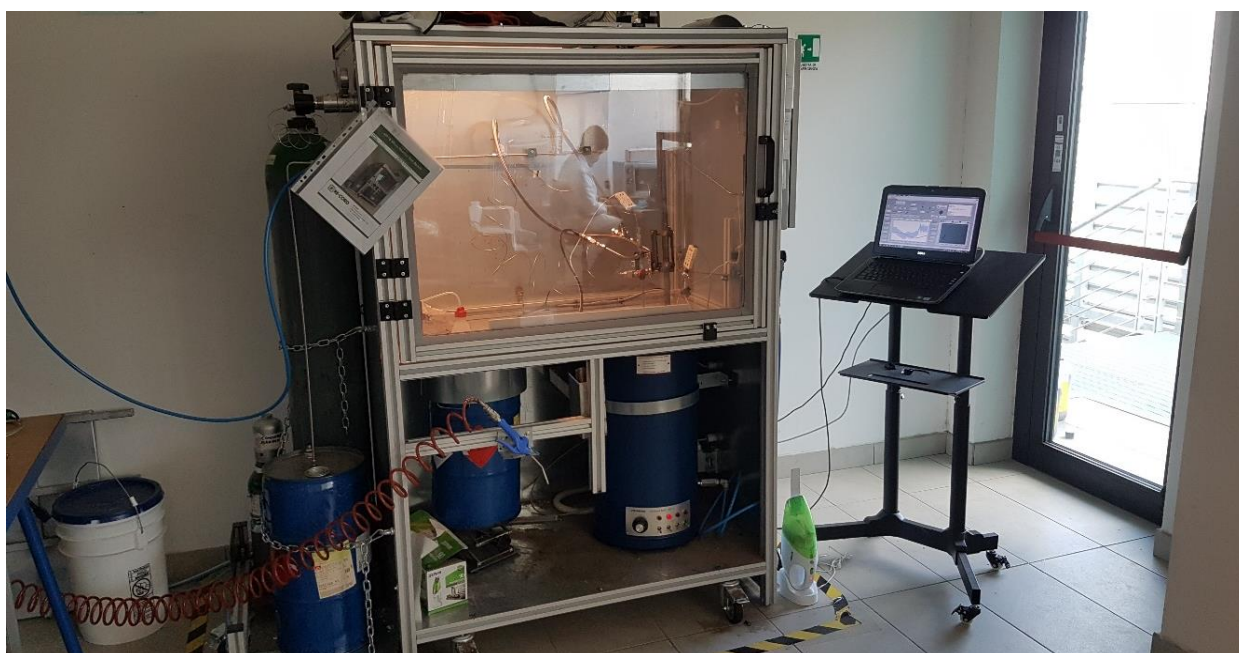


Figure 23: Micro Reactor Test-Bench at RE-CORD' laboratory.

The sand bed of the MRTB is fluidised by means of compressed air at +0.2 bar, with a flow rate at 68 l/min; it is always kept on to avoid the resistors overheating. The MRTB system also has the following utilities:

- N₂ cylinder with a pressure range of 0-6 bar.
- Ar cylinder with a pressure range of 0-200 bar, used for leakage tests.
- Barrel of distilled water at 20 °C to quenching of reactor.
- Other utilities to obtain gas as He, H₂, etc.
- An electric motor to keep moving the reactor during the experiments.

Sand temperature, pressure and temperature inside the reactor are continuously monitored by means of a National Instrument Data Acquisition System (NI-DAQ). It monitors and saves any data that the sensors collect. Three sensors are present to capture data: two temperature sensors (both PT100, 3-wire RTD temperature sensor, B accuracy class), where the first is located in the bottom of the fluid sand bed, and the second one on the external metal surface to measure the temperature the reactor temperature; third sensor is inside the reactor to monitor the mid reaction temperature. The scheme of the MRTB system is shown in Figure 24.

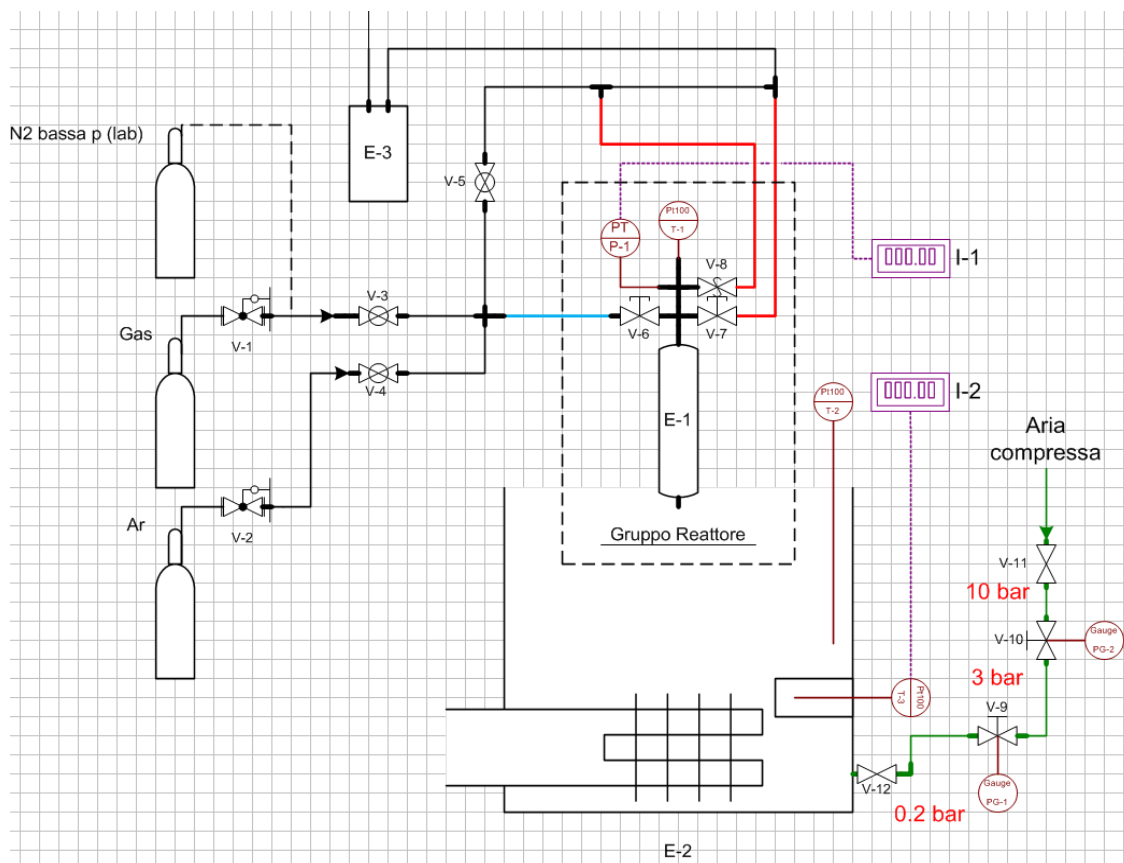


Figure 24: Micro Reactor Test-Bench (MRTB) scheme.

The reactor consists in a 300 mm-long AISI 316 $\frac{3}{4}$ -inch tube (outer diameter), modified with Swagelok fittings. It is equipped with a PT100, a 3-wire RTD temperature sensor (1/10 DIN accuracy class), a pressure transducer and a pressure relief valve for safety depressurization. The reactor is formed by three parts as shown in Figure 25: a top, a bottom and a tube. When it closes, it has 42 ml of volume. The maximum allowable pressure for the reactor is 170 bar.

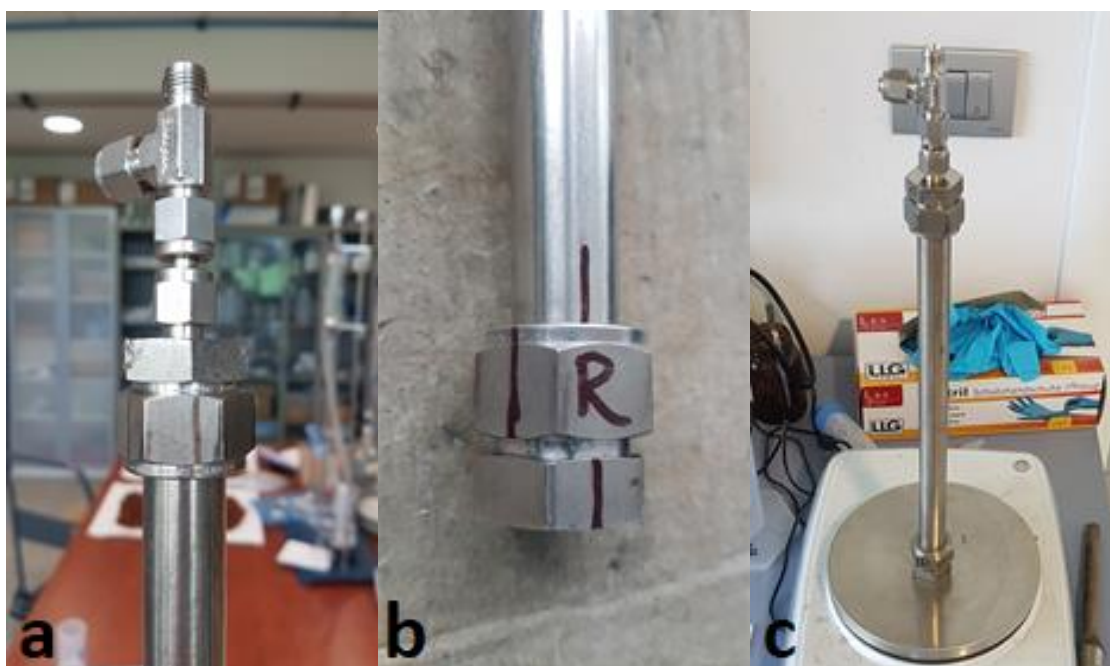


Figure 25: Experimental reactor: a) Top; b) Bottom; c) Reactor complete.

5.3 Methods for MRTB tests, collection of product and titration

5.3.1 Deoxygenation tests

All deoxygenation experiments followed the same procedure according to the following steps:

1. A clean reactor, weighed (bottom, tube and top) and then was reassembled. The reactor was loaded with 13.7 g stearic acid; subsequently the reactor sealed off and was weighed again.
2. Pressure and temperature sensors were connected to the reactor and the reactor was sealed off.
3. A leakage test was carried out with Ar in the pressure range of about 40-80 bar (in these experiments the pressure was not very high, so the leakage test was carried out in that pressure range). If there were leaks, nuts were tightened more until there were no more leaks.
4. Reactor was purged with N₂ three times to remove the presence of oxygen inside.
5. The reactor was immersed in the sand bed and when the internal temperature reached the set temperature, the reaction started for 30 minutes. Temperature was monitored to remain constant for the entire reaction time.
6. After 30 minutes, the reactor was removed from the sand bed, compressed air was blown over the reactor to remove sand residues, and immediately after that, the reactor was inserted into the barrel of distilled water to quench for 20 minutes.
7. After 20 minutes, the reactor was removed from the barrel and was depressurized.
8. The reactor was disconnected from MRTB and subsequently was weighed again.
9. The reaction product was transferred to a vial followed by weight measurement.
10. Subsequently the reaction products were transferred to the laboratory for a further analysis (according to the methods explained in Feedstock and methods of analysis).
11. The reactor was weighed again before washing.

5.3.2 Hydrolysis tests

The procedure is similar to the decarboxylation experiments with different reaction conditions. In this experiment, 22.05 g of glycerol trioleate was mixed with 9 g of ultrapure water inside the reactor (41 % w/w water to oil mass ratio). A leakage test was performed by Argon pressurization at 80 bar and air was then removed with five purging cycles with Nitrogen at 5 bar. After these preliminary operations, the reactor was pressurized with Argon at the chosen initial pressure of 40 bar and subsequently immersed into the hot fluidized bed. When the reactor temperature reached the set point (230 °C), computing of the residence time started and the reactor was kept there for the desired time (2 hours). Once the time had elapsed, the reactor was removed from the sand bed, sand residues were removed with pressurized air and immediately after immersed in the water barrel for rapid cooling. After 20 minutes, the reactor was removed from the water barrel and the pressure released.

To measure the amount of free fatty acids released by this test, the reactor content was transferred to a decanter (Figure 26). Subsequently, after the separation of the heavy reaction products (water and glycerol) and the light reaction products (free fatty acids and unconverted triglycerides) a titration was carried out on the light reaction products and on the initial feedstock (glycerol trioleate) with the same procedure used for the decarboxylation reaction products.

Subsequently the reaction product and the initial reactor content were put in a refrigerator at 1.5 °C for 24 hours.



Figure 26: Separation of the heavy and lighter phase for analysis by decanter.

5.3.3 Sample collection

After each test, the reaction products were collected in a vial. Depending on reaction conditions, the product was solid, solid and liquid or almost completely liquid. In case of a solid product, it was crushed to create a homogeneous mix in order to execute a more correct titration (Figure 27). If the reaction product was solid and liquid, the products were separated and subsequently a centrifuge was executed on the liquid product; then the liquid product was collected in a vial with a 1 ml pipette and the solid and liquid products were weighed. Finally, if the reaction product was almost completely liquid, then a centrifuge was directly carried out and subsequently the liquid product was separated with a 1 ml pipette in a vial. Finally, the liquid product and its solid residues were weighed. Each centrifuge was carried out at 4100 rpm for 5 minutes at 20 °C.



Figure 27: Crushed (a) and collected (b) of solid product.

5.3.4 Titration

Immediately after sample collections, the main analytical procedure carried out was titration. This procedure consists in the calculation of the number of acidity, that is fundamental to understand the decarboxylation degree of the product before other reactions (e.g. aging) can occur. To calculate the number of acidity the following steps were followed:

1. Base preparation (KOH) with a mix of 1.40 g of Potassium Hydroxide and 250 ml of Ethanol (both produced by Sigma-Aldrich).
2. Solvent preparation for normalization, standardization and FA solution: mix 1:1 of Ethanol and Diethyl Ether (produced by Sigma-Aldrich).
3. Solvent neutralization: three drops of phenolphthalein were added in the solvent and after add KOH until it changes colour (becomes pink).
4. Solvent standardization: 10 ml of Hydrochloric Acid and 50 ml of solvent and three drops of phenolphthalein were mixed; subsequently KOH was added until the solution changed the colour. A triplicate was done for all samples at this step.
5. Determination of acidity number (both for stearic acid and for the reaction product). about 0.20 g of feedstock (or reaction product) and after add 75 ml of solvent were mixed three drops of phenolphthalein. KOH was added until the solution changed colour. Figure 28 shows the solution before and after adding of KOH. A triplicate was performed for step 5 as well. In addition, absolute standard deviation and confidence interval at 95 % confidence level were determined.

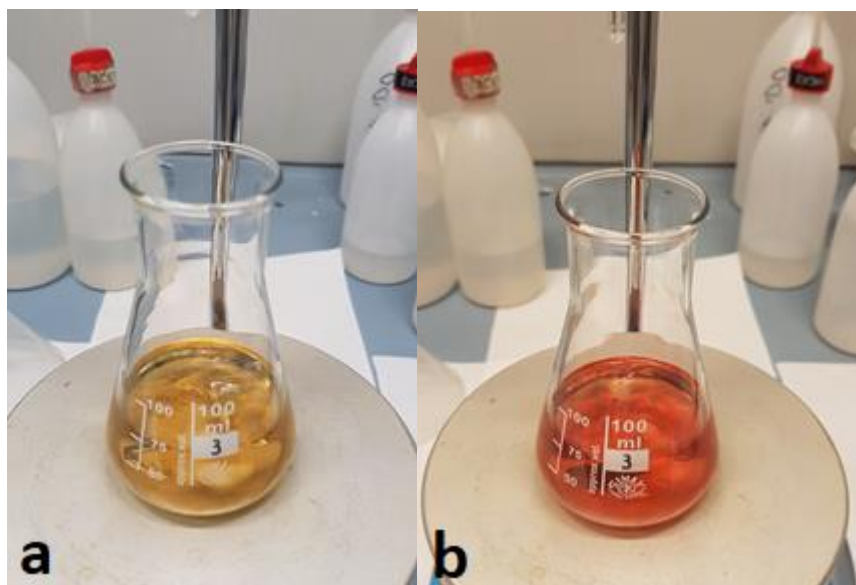


Figure 28: Determination acidity number: colour of solution before (a) and after (b) KOH adding.

After titration tests, it is possible to calculate the acid value of the reaction products. Therefore, the deoxygenation degree is calculated (DOX %) as:

$$\text{DOX \%} = \frac{\text{Acidity number}_{\text{feed}} - \text{Acidity number}_{\text{prod}}}{\text{Acidity number}_{\text{feed}}} \cdot 100$$

In conclusion, samples have been analysed through GC methods, according to the procedure reported in paragraph Feedstock and methods of analysis.

5.4 Design of experiments

In total, thirteen experiments were executed with the tubular reactor in the Micro Reactor Test-Bench (MRTB), in which twelve were carried out to study the deoxygenation of stearic acid and one to study hydrolysis of glycerol trioleate. The stearic acid thermal cracking was carried

out at 300, 320, 340, 360, 380, 400, 420, 430, 440, 450, 460, 470 °C in N₂ atmosphere, always with the same initial pressure of 0.1 bar and always with a reaction time of 30 minutes at constant temperature. Each test was carried out without a catalyst. All the reaction products were collected and analysed to figure out the reaction mechanism underlying thermal cracking of fatty acids.

6. Experimental campaign: results

6.1 Feedstock

As first, in order to study the initial feedstock, three batches of UCO from different origins were analyzed and results reported in Table 1.

Table 5: UCO batches supplied from SILO SpA (Florence, Italy).

Parameter	Unit	Method	RES.18.022_018	RES.18.022_019	RES.18.022_020
			SILO UCO from fast foods	SILO UCO from restaurants	SILO UCO (OLLI) from domestic collection
Kinematic Viscosity at 40 °C	mm ² s ⁻¹	UNI EN ISO 3104	38.03	34.96	31.39
Acid value	mg _{KOH} g ⁻¹	UNI EN 14104	8.2	0.9	1.6
Free Fatty Acid	%wt	ISO 660	4.1	0.5	0.8
Water content	%wt	UNI EN ISO 8534	0.8	0.2	1.6
Ash	%wt	UNI EN ISO 6245	0.01	u.d.l.	0.01
Total contamination	mg kg ⁻¹	UNI EN 12662	903	731	1249
Sulphur	mg kg ⁻¹	Internal method	u.d.l.	u.d.l.	u.d.l.
C	%wt	ASTM D 5291	76.0	76.1	76.5
H	%wt	ASTM D 5291	11.3	11.2	11.4
N	%wt	ASTM D 5291	0.1	0.1	0.1
O	%wt	Calculated	12.6	12.6	12.0
Calorific value, higher	MJ kg ⁻¹	DIN 51900-2	39.09	39.34	38.94
Calorific value, lower	MJ kg ⁻¹	Calculated	36.63	36.89	36.45

All of three batches exhibit slightly different properties as result of their origins. In particular, UCO from fast food is more viscous and acid, the result of a more intense saturation and use. Domestic UCO appears as the richest in contaminations (solids) since it traps more residues from cooking processes due to its use in small pots. UCO from restaurants is the cleanest one among the samples, and moreover is shows the higher energy content probably due to a lower water content.

6.2 Hydrolysis tests

The hydrolysis experiment was carried out in the micro reactor at an operating temperature of 230 °C and an initial pressure of 40 bar of Argon as well as 2 h of reaction time. Glycerol Triolate was used as a model molecule of triglycerides. Molar ratio of 47.1 wt% (water-to-oil, 20:1 in mass) was selected on the basis of Stephen John Reaume's paper [68], and his results in Figure 29.

Temperature (°C)	Pressure (MPa)	Catalyst	Time (h)	Conversion (wt%)
100	0.0	H ₂ SO ₄	1	0
100	0.0	H ₂ SO ₄	2	2
100	0.0	H ₂ SO ₄	4	5
100	0.0	H ₂ SO ₄	6	16
150	1.0	N/A	4	2
170	2.0	N/A	4	21
190	2.5	N/A	4	47
210	3.0	N/A	4	74
230	4.0	N/A	4	98
250	5.0	N/A	4	98
270	6.0	N/A	4	98
230	4.0	N/A	1	87
230	4.0	N/A	2	98
230	4.0	N/A	6	98

Figure 29: Study on optimization of hydrolysis (all trials were done with molar ratio 20:1) [68].

According to this scheme, the object of test was to study the penultimate condition. Our experimental test showed a good separation of fatty acids from glycerol via hydrolysis, as shown in Figure 26. Free fatty acid content was measured by 2 triplicates. First triplicate was aimed to measure free fatty acid content in the initial feedstock, while in the second run in the product. By means of the titration procedure for initial feedstock (glycerol trioleate), and the hydrolysis product, the number of acidity was calculated. Calculating the difference of the number of acidity between the initial feedstock and the hydrolysis product, it has been calculated the increased fatty acids content. Results are shown in the following Table 6.

Table 6 Analysis of the feedstock (GO, Glycerol Trioleate) and the product (hydrolysis experiments).

	Number of acidity [mg/g]	Average [mg/g]	Free fatty acid content (wt.%)	Average (wt.%)	Increase of FFA content (wt.%)
GO (sample A)	3.12	2.77	1.56	1.39	27.76
GO (sample B)	2.68		1.34		
GO (sample C)	2.52		1.26		
Product (sample A)	57.5	58.29	28.75	29.15	
Product (sample B)	57.86		28.93		
Product (sample C)	59.52		29.76		

The results from the titration showed that in the hydrolysis process an increase of free fatty acids content occurred with a 27.76 wt.%. Moreover, a change in color of the heavy phase and light phase was observed as shown in Figure 30: vial on the left side shows the combination of feedstock and water with water to oil ratio of 20:1 before the reaction, and the decanter on the right side shows the content of the reactor after the hydrolysis process.

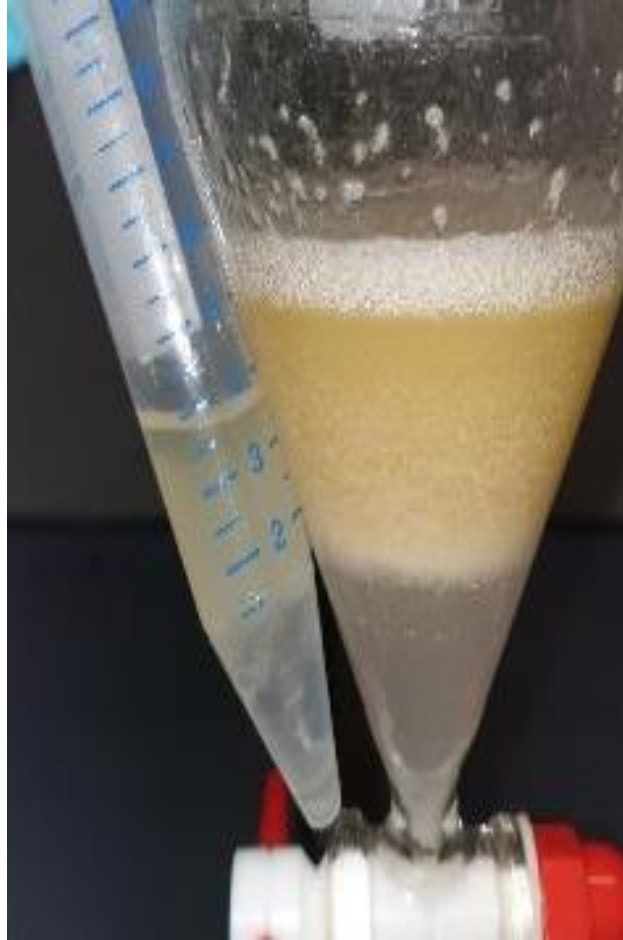


Figure 30: The vial on the left side contains the reactor content before reaction; the decanter collects the reaction product.

A vial containing the reaction product was then put inside a refrigerator at 1.5 °C along with the vial containing a mixture of feedstock and water. After 24 hours, they were taken out and checked. The vial containing glycerol trioleate had been solidified, while the vial including the products of the reaction was still in the liquid phase, as shown in Figure 31.

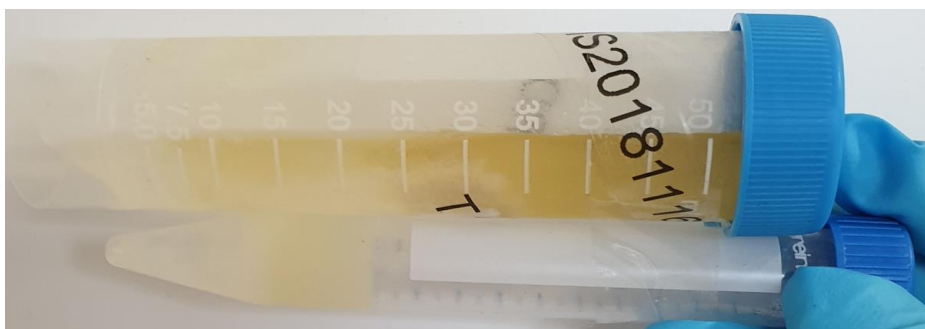


Figure 31: Vials after one day in the refrigerator at 1.5°C.

This procedure validated the hydrolysis experiment since the melting point decreased, due to the splitting of the triglyceride and the subsequent presence of fatty acids and glycerol. The lower conversion rate than the work of Stephen John Reaume [68] was probably due to the lack of agitation in this experiment.

6.3 Deoxygenation tests

As the second phase of the experimental activities, a set of experiments were carried out from 300 to 470 °C without catalysts. The temperature was selected as the main parameter to change the reaction conditions. The reaction time was set as 30 min for every test. Micro reactor was initially pressurized to 5 bar N₂ and purged three times before the heating ramp up. Heating rate was 80 °C/min. Figure 32 depicts the samples after extraction from the micro reactor.

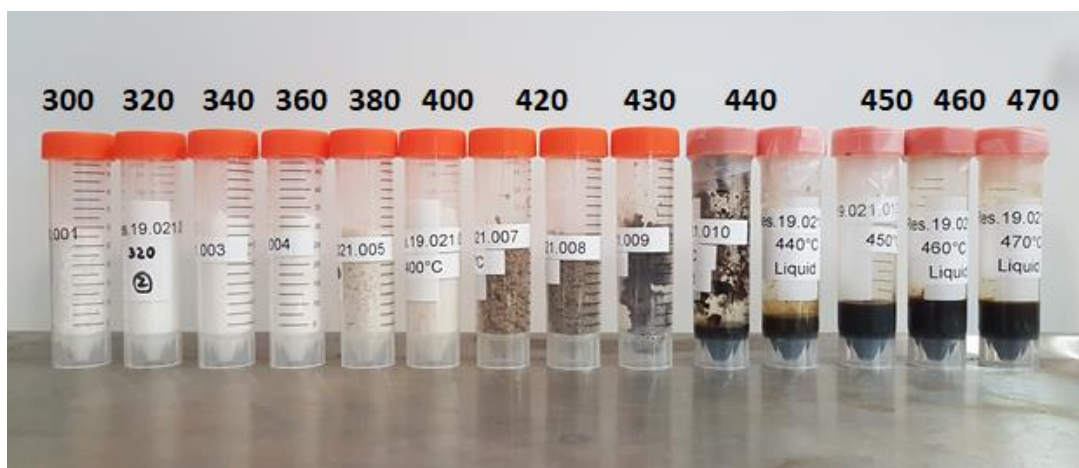


Figure 32: The reaction products collected in vials, ordered from the lowest to the highest temperature.

6.3.1 Effect of reaction temperature and heating rate

With the temperature change, the other parameters of the reaction changed significantly, in particular the maximum pressure and the heating rate, as shown in the following graphs (respectively Figure 33 and Figure 34).

Figure 33: A diagram showing the maximum pressure in function of the reaction temperature per test.

The maximum pressure increases significantly with the temperature increase. As Figure 33 shows, it slightly changes from 300 to 400 °C where it increases from 1.9 at 5.47 bar, while it presents an exponential growth starting at 420 °C where it reaches the maximum of 85.14 bar at 470 °C. From 300 to 400 °C, the maximum pressure increases of almost 3 times, while from 400 to 470 °C is increases of almost 16 times. Also, Maher and Bressler [29] observed the increase of maximum pressure with the reaction temperature growth. The reasons of the maximum pressure increase can probably be attributed to the production of lighter compounds due to cracking of the mother molecule, cracked fatty acids and, decarboxylated hydrocarbons: a higher temperature allows the cracking of stearic acid, that occurs over 420 °C. At temperatures over 420 °C, more initial feedstock reacts, with a consequent increase of gas production.

Figure 34: Heating rate increase in function of reaction temperature.

Clearly heating rates increased with increasing reaction temperature (Figure 34). The fluctuations present at 380 and 420 °C are due to the absence of controlled temperature ramp up in the MRTB electrical board. However, the scope of this work was to heat up the reactor faster than traditional TGA, which operates in the range 1-25 °C/min. Some authors [2] attribute lower liquid conversion yield when high heating rates (> 15 °C) are used, but our results are in line with Guedes' work [69], that remarked a minor influence of the heating rate on the reaction than temperature or pressure at relatively long residence time (i.e. from minutes to hours).

6.3.2 Conversion yield

Stearic acid is solid at ambient temperature, while hydrocarbons are liquid. The effect of thermochemical conversion changed the state of aggregation of feedstock, indicating in the form of the product the effect of thermal cracking. When reaction temperature increased, the remaining solid product (unconverted stearic acids) decreased, while the liquid and gas product increased too. In the following graphs, the conversion yield of the final products is observed in function of the reaction temperature.

Figure 35: a) wt.% Recovered product in function of T; b) wt.% Solid product in function of T; c) wt.% Liquid product in function of T; d) wt.% Gas product in function of T.

In Figure 35 a) the mass fraction of reaction products collected after each test is reported. In Figure 35 b), c) and d) respectively, the solid, liquid and gas yield of the reaction product collected are shown. The gas product was calculated as a weight loss between the weight of initial feedstock and the weight of the collected product. As Figure 35 depicts, when temperature increases, the fraction of the solid recovered reaction product decreases, and in parallel, the fraction of the solid product decreases, while the percentage of the liquid and the gas product increases.

Table 7: Mass distribution of products under the various temperature conditions.

Reaction Temperature	Solid	Liquid	Gas
°C	wt%	wt%	wt %
300	99	0	1
320	99	0	1
340	99	0	1
361	99	0	1
380	98	0	2
401	98	0	2
420	94	0	6
430	88	0	12
440	46	39	15
450	4	81	15
460	4	76	19
470	4	67	29

In particular, from 300 to 400 °C, the reaction products are composed by the only solid fraction that is just unreacted feedstock (as shown in Table 7). In this temperature range, a gradual reduction of the recovered product percentage (that is only solid) and a gradual increase of the percentage of gas product occurred. Moreover, at 420 and 430 °C, the reaction products were still solid, but they started to become darker and wetter (Figure 36). At temperatures higher than 430 °C, a rapid increase of gas fraction occurred, reaching the maximum percentage in weight of 26.9 % at 470 °C. This observation is in agreement with the maximum pressure increase, which resulted for the high gas fraction produced.

300-360°C



380-400°C



420°C



430°C



Figure 36: Reaction products at different set test temperatures between 300 and 470 °C.

From 440 °C onwards, the liquid fraction started to be present in the reaction product, and in parallel, a slight decline in the solid fraction occurred. At 440 °C, the percentage of liquid fraction was almost the same of solid fraction. At 450 °C, the reaction product was completely liquid, with only a small part of solid residue that persisted (lower than 5% of the recovered product). At this temperature, the maximum liquid yield of the entire set of experiments was obtained. At 460 and 470 °C, the process was gradually inverted: the liquid fraction decreased, while the solid residue slowly increased.

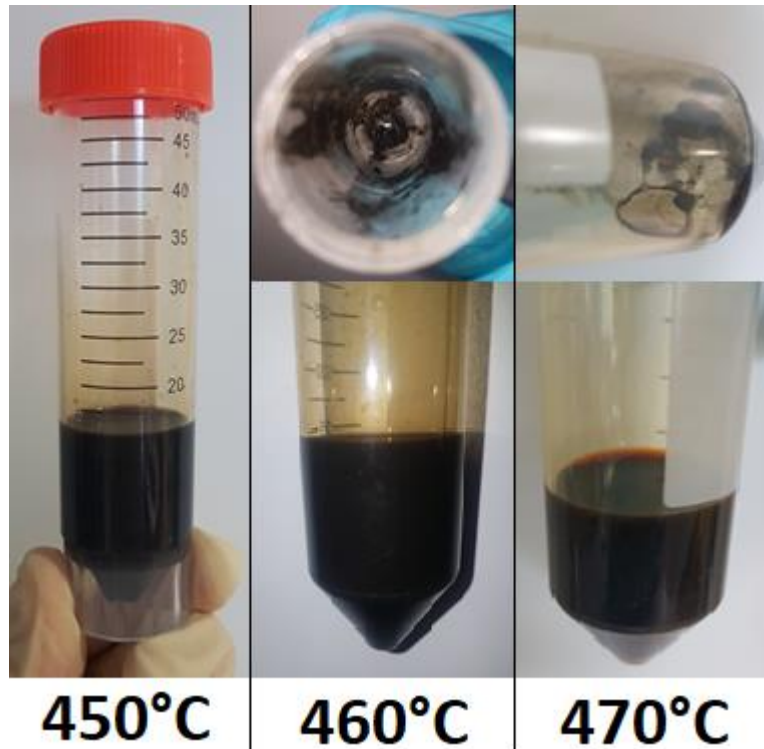


Figure 37: Reaction products at 450, 460 and 470°C.

This result is due to the increase of the cracking degree: the higher temperature breaks the stearic acid molecules into shorter molecules and after the quenching, remain in the gaseous form, with a consequent decrease of the liquid fraction and an increase of the gas product, as shown in Figure 35. The higher temperature caused a first formation of carbonaceous deposits as Figure 37 illustrates: the presence of char could have the function of a catalyst that accelerates the kinetics of the reaction, leading to a reduced final product liquid yield. At 470 °C, Figure 37 depicts the presence of water in small amounts. This suggests that a part of the deoxygenation reaction has occurred by decarbonylation (DCO) as shown in Figure 4. The water is a side product and at the same time an indication of the stearic acid deoxygenation. The presence of water lowers the bio-oil calorific value, while a target potential decarboxylation reaction (DCO₂) would produce carbon dioxide, which does not influence the energy content of the final products.

6.3.3 Acidity and deoxygenation degree

The result of the titration tests let to calculate the deoxygenation degree (DOX %), as reported in Figure 38. The error bars indicate the confidence interval evaluated at 95 % confidence level.

Figure 38: Deoxygenation degree (DOX %) in function of temperature; error bars indicate the confidence interval.

The graph shows that until 400 °C, the deoxygenation reaction does not start, in agreement with the experiments of Sim et al [28]. In the temperature range between 420 and 440 °C, an exponential growth of DOX % occurs and reaches the maximum at 66.02% for 460 °C. At 450 °C, there is an uncertain decline, likely due to the presence of solid residues (unreacted initial feedstock) in the samples of the titration. At 470 °C, the DOX % starts to gradually decrease but always remains higher than 60%. These results are in agreement with the previous graphs, which show the weight percentage of the solid, liquid and gas fraction of the collected reaction products. Based on these experiments, it has not been possible to obtain a deoxygenation degree over 70 % with a deoxygenation reaction in a batch reactor without the

use of catalysts. The results show a low standard deviation, which causes a restricted confidence interval; this is an indication of a good reliability of the obtained results.

6.3.4 Hydrocarbons quantification

By means of Gas Chromatography techniques, the main constituents of the reaction products were quantified. The chromatograms are shown in Figure 39, while the quantification of products is reported in Table 8. The evidence of target deoxygenation reaction is the presence of heptadecane hydrocarbon C17, in agreement with the results of Maher and Bressler [29]. Based on the results, as already evident in Figure 35 and Figure 38, in the temperature range between 300 and 380 °C, the stearic acid was not converted. In fact, it is the only peak present in the GC graph. The first traces of heptadecane are present at 400 °C. At 420 °C, the peak of the graph indicates that the main element in the reaction product is heptadecane that confirmed the decarboxylation reaction of stearic acid. There other lower peak showed the unconverted stearic acid. At 430°C, the main product is still heptadecane, while the peak of stearic acid is gradually reduced in favour of other hydrocarbons conversion. From 440 °C onwards, the analysed product is separated into a solid and liquid part, and all chromatograms show a similar trend. From the quantification of hydrocarbons in Table 8 emerges that the test at 450 °C converted up to 64% of stearic acid in hydrocarbons, where 25% is C17. In addition, Figure 39 illustrates an excellent selectivity towards linear alkanes as 8 peaks before stearic acid peak. Increasing temperature above 450°C, the cracking reactions are too much intense and the target deoxygenation of carboxylic group is reduced in favour of generic cracking reactions along stearic acid chains, that led to higher gas production. This phenomenon has been confirmed measuring the oxygen content of the sample produced at 470 °C, which has higher oxygen content that the sample produced at 460°C. This result is in agreement with the outcomes from literature review of Chapter **Literature review**, since a higher temperature produces a higher number of cracking points along fatty acids molecules, with a consequent increase of volatility and pressure.

The significant presence of heptadecane confirmed that deoxygenation (in particular decarboxylation) reaction occurred. The absence of water in samples at 420 and 430 °C suggests that, the deoxygenation reaction occurs mostly through the decarboxylation pathway. With the temperature and pressure increase, the decarboxylation reaction becomes more significant.

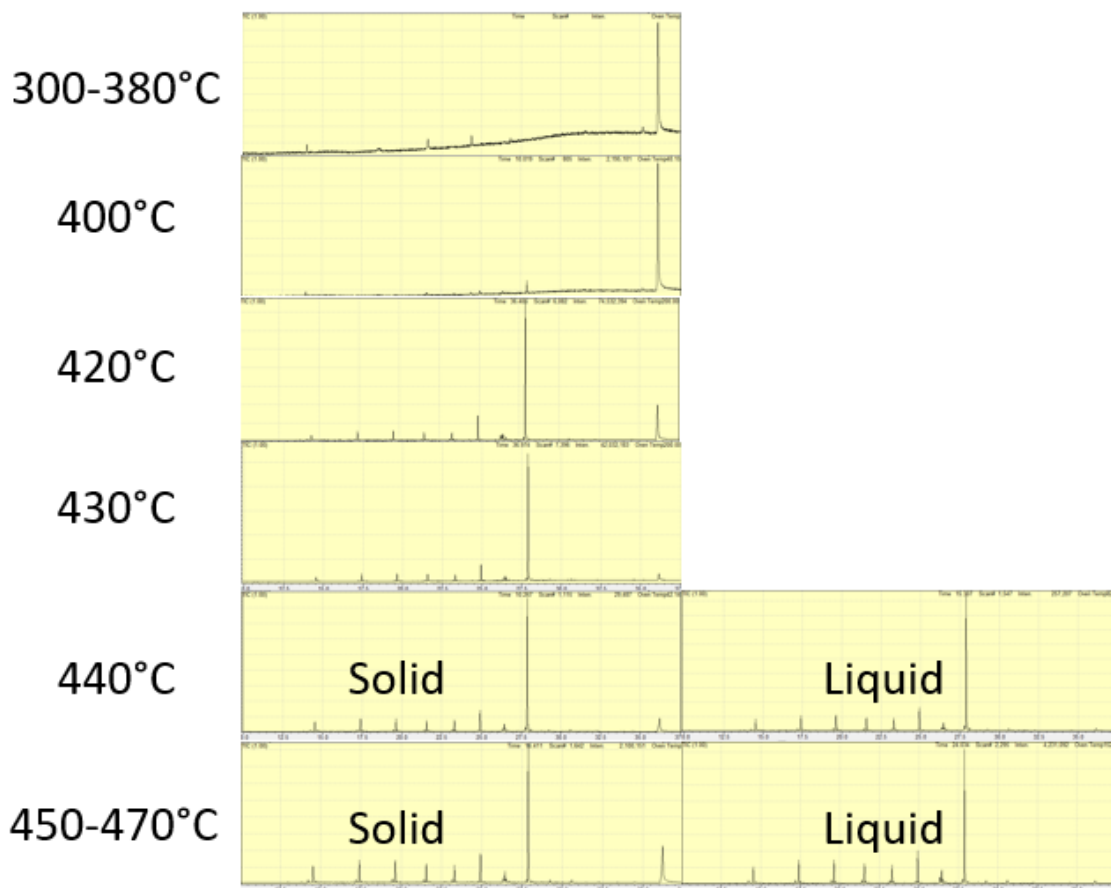


Figure 39: GC results for each reaction product collected.

Table 8: Results from GC quantification of hydrocarbons.

Test nr.	T(°C)	t(min)	Acidity (mg di KOH)	DOX%	Oxygen (w/w%)	C17 (w/w%)	C7/C38 (w/w%)	C18:0 (w/w%)
1	300	40	194	0	11	0	0	96
2	320	40	199	0	9.9	0	0	85
3	340	40	196	1.1	9.5	0	0	84
4	360	40	196	2.2	9.3	0	0	90
5	380	40	198	2.2	8.8	0	0	67
6	400	40	187	4.8	9.6	0	0	81
7	420	40	157	20	8.1	12	12	75
8	430	40	125	37	5.4	20	20	60
9	440	40	107	62.5	5.1	17	27	19
10	450	40	105	57	5.2	25	64	10
11	460	40	146	66.5	3.9	11	40	9
12	470	40	127	65	4.3	4	34	5

6.3.5 Discussion

The proposed R&D campaign for lipid pre-processing before HVO confirmed that the deoxygenation reaction can occur without using hydrogen and catalysts. The effect of temperature, heating rate, reaction time and fatty acids species strongly affect the target cracking process in proximity of the oxygen bonds to favour deoxygenation reactions to produce hydrocarbons. In the range between 300 and 470 °C as reaction temperature, it has been observed that cracking process through a batch pressurized thermochemical conversion starts above 400°C. However, for a fixed reaction time of 30 minutes, a sufficient deoxygenation degree starts from 420 °C onwards. Probably, with an increase of residence time, the deoxygenation process could already start at 400 °C or less, as verified by Sim et al [28] for saturated fatty acids. Differently, if these tests would be carried out with an unsaturated fatty acid, the reaction starts at lower temperatures, as reported by Sim et al [28]. At higher temperatures, a higher volatilization of the initial feedstock happens (compared to saturated fatty acids), with a consequent pressure increase: in these reaction conditions, the deoxygenation process occurs through decarboxylation until 450-460 °C. At 470 °C, the presence of water, suggests that part of the reaction undergoes through the decarbonylation process. Asomaning et al [27] observed a predominant deoxygenation reaction of oleic acid from 430 °C, while at higher temperatures, it remained constant promoting in parallel the decarboxylation reaction. This fact is probably due to the higher grade of volatilization of unsaturated fatty acids, which led to higher reaction pressure that favours the reaction even at lower temperature. In the present tests with a saturated fatty acid as feedstock, when at 420 °C the deoxygenation process occurs, the absence of water in both samples at 420 and 430 °C suggests that conversion to C17 is performed through the decarboxylation reaction. Subsequently, with the temperature increase (and consequent pressure increase), the deoxygenation reaction occurs also through the decarbonylation pathway. A full stearic conversion to C17 is not possible, but the optimum conditions with the proposed layout has been observed at 450 °C as shown in Figure 40. This result is a compromise with the above-mentioned phenomena. At this temperature, a realistic hypothesis is a more intense decarbonylation process at higher pressure, based on the results of the experiments over 50 bar.

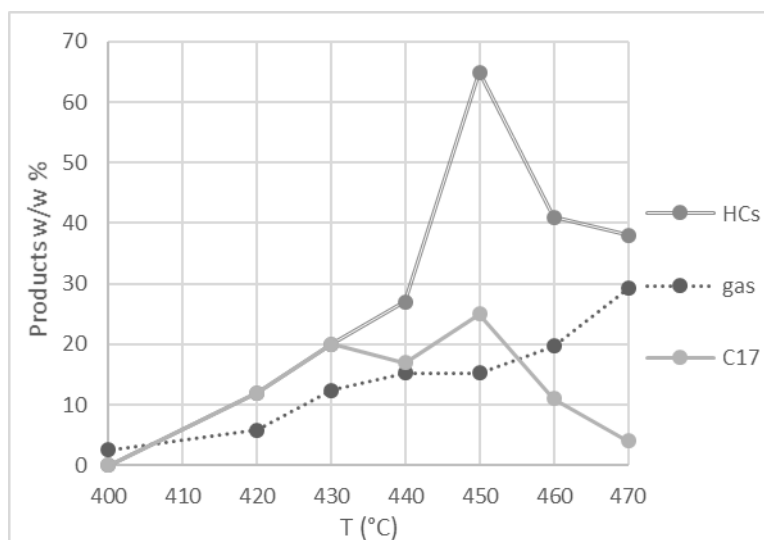


Figure 40: Elaboration of results from Table 8.

6.3.6 Conclusions

The present report investigated R&D pre-treatment strategies for waste lipids before HVO process. The aim of the work was to reduce the overall hydrogen demand and high-priced catalysts used in the HVO process to produce bio-hydrocarbons. The investigated preliminary pre-treatment step for waste lipids consists in a first hydrolysis of tryglicerides to produce pure

and saturated fatty acids, which are then partially converted in n-paraffins through a simple pressurized thermal conversion.

In total, thirteen experiments were performed with a tubular reactor in the Micro Reactor Test-Bench (MRTB), in which twelve were carried out to study the deoxygenation of stearic acid and one to study hydrolysis of glycerol trioleate. The stearic acid thermal cracking was carried out at 300, 320, 340, 360, 380, 400, 420, 430, 440, 450, 460, 470 °C in N₂ atmosphere, always with the same initial pressure of 0.1 bar and always with a reaction time of 30 minutes at constant temperature. Each test was carried out without a catalyst. All the reaction products were collected and analysed to figure out the reaction mechanism underlying thermal cracking of fatty acids.

The best result was achieved in the test at 450°C, obtaining a liquid yield of 81% (as mass fraction) containing up to 64% (in mass) of hydrocarbons (where 25% is n-heptadecane).

At the second phase of the project, high pressure non-catalytic conversion was selected to convert the fatty acids in n-paraffins. Therefore, for this step, stearic acid was selected as a saturated long chain fatty acid as a model compound, to study the desired temperature for decarboxylation and therefore hydrocarbon production. An important adopted strategy was using high pressure that promotes production of more saturated hydrocarbons [16][29]. High pressure hinders evaporation of alkenes as well as unsaturated cracked fatty acids from migrating to the vapor phase. As such, they react with the formed radicals in the liquid phase as the activation energy for this reaction is quite low 2-8 kcal/mole [16]. In addition, high pressure, shifts the equilibrium reaction of aromatization and cyclization towards left i.e. maximizing selectivity towards linear alkanes. The result, in this case, is expected to be a highly selective process mostly producing paraffines and isoparaffines.

For the future the experimental plan will focus on catalytic deoxygenation. The catalysts of choice will be microporous heterogeneous solid acids known as zeolites. These catalysts are environmentally friendly, their rate of deactivation is low, and they are easily recoverable. They change their properties depending on the size of the pores as well as silica to alumina ratio. These catalysts are commercially available and have the ability to be doped with different metals for the research and the industry. Using these catalysts, a higher conversion yield and a higher quality liquid product can be produced with the proposed HVO preliminary pre-treatment strategy.

6.3.7 Bibliography/References

- [1] Ling T, Chang J, Chiou Y, Chern J. Journal of Analytical and Applied Pyrolysis Characterization of high acid value waste cottonseed oil by temperature programmed pyrolysis in a batch reactor. *J Anal Appl Pyrolysis* 2016;120:222–30. <https://doi.org/10.1016/j.jaap.2016.05.009>.
- [2] Ben A, Trabelsi H, Zaafour K, Baghdadi W, Naoui S. Second generation biofuels production from waste cooking oil via pyrolysis process. *Renew Energy* 2018;126:888–96. <https://doi.org/10.1016/j.renene.2018.04.002>.
- [3] Chen G, Liu C, Ma W, Zhang X, Li Y, Yan B, et al. Bioresource Technology Co-pyrolysis of corn cob and waste cooking oil in a fixed bed. *Bioresour Technol* 2014;166:500–7. <https://doi.org/10.1016/j.biortech.2014.05.090>.
- [4] Xu J, Jiang J, Zhao J. Thermochemical conversion of triglycerides for production of drop-in liquid fuels. *Renew Sustain Energy Rev* 2016;58:331–40. <https://doi.org/10.1016/j.rser.2015.12.315>.
- [5] Kulkarni MG, Dalai AK. Waste Cooking Oil s An Economical Source for Biodiesel : A Review 2006:2901–13. <https://doi.org/10.1021/ie0510526>.
- [6] Chang J, Cheng J, Ling T, Chern J. Journal of the Taiwan Institute of Chemical Engineers Low acid value bio-gasoline and bio-diesel made from waste cooking oils using a fast pyrolysis process 2017;73:1–11. <https://doi.org/10.1016/j.jtice.2016.04.014>.
- [7] Sannita E, Aliakbarian B, Casazza AA, Perego P, Busca G. Medium-temperature conversion of biomass and wastes into liquid products, a review. *Renew Sustain Energy Rev* 2012;16:6455–75. <https://doi.org/10.1016/j.rser.2012.06.017>.
- [8] LET'S MAKE BIODIESEL. TaboodadaWordpressCom 2012.
- [9] Eduardo E, Fernando E, V MC. Biomass and Bioenergy Hydrotreatment of vegetable oils : A review of the technologies and its developments for jet biofuel production 2017;105. <https://doi.org/10.1016/j.biombioe.2017.07.008>.
- [10] Choi I, Lee J, Kim C, Kim T, Lee K. Production of bio-jet fuel range alkanes from catalytic deoxygenation of Jatropha fatty acids on a WO_x / Pt / TiO₂ catalyst G R A P H I C A L A B S T R A C T. *Fuel* 2018;215:675–85. <https://doi.org/10.1016/j.fuel.2017.11.094>.
- [11] Santillan-jimenez E, Morgan T, Lacny J, Mohapatra S, Crocker M. Catalytic deoxygenation of triglycerides and fatty acids to hydrocarbons over carbon-supported nickel. *Fuel* 2013;103:1010–7. <https://doi.org/10.1016/j.fuel.2012.08.035>.
- [12] Asikin-mijan N, Lee H V, Juan JC, Noorsaadah AR, Chyuan H, Razali SM. Applied Catalysis A , General Promoting deoxygenation of triglycerides via Co-Ca loaded SiO₂-Al₂O₃ catalyst 2018;552:38–48. <https://doi.org/10.1016/j.apcata.2017.12.020>.
- [13] Fréty R, Pacheco JGA, Santos MR, Padilha JF, Azevedo AF, Brandão ST, et al. Journal of Analytical and Applied Pyrolysis Flash pyrolysis of model compounds adsorbed on catalyst surface : A method for screening catalysts for cracking of fatty molecules. *J Anal Appl Pyrolysis* 2014;109:56–64. <https://doi.org/10.1016/j.jaap.2014.07.013>.
- [14] Li D, Xin H, Du X, Hao X. Recent advances for the production of hydrocarbon biofuel via deoxygenation progress 2015;60:2096–106. <https://doi.org/10.1007/s11434-015-0971-0>.
- [15] Krobkrong N, Itthibenchapong V, Khongpracha P. Deoxygenation of oleic acid under an inert atmosphere using molybdenum oxide-based catalysts. *Energy Convers Manag* 2018;167:1–8. <https://doi.org/10.1016/j.enconman.2018.04.079>.
- [16] Khorasheh F, Gray MR. High-pressure Thermal Cracking of n-Hexadecane 1993:1853–63. <https://doi.org/10.1021/ie00021a008>.
- [17] Sadighi S, Zahedi S, Hayati R, Bayat M. Studying Catalyst Activity in an Isomerization Plant to Upgrade the Octane Number of Gasoline by Using a Hybrid Artificial-Neural-Network Model. *Energy Technol* 2013;1:743–50. <https://doi.org/10.1002/ente.201300104>.
- [18] Maher KD, Bressler DC. Pyrolysis of triglyceride materials for the production of

-
- renewable fuels and chemicals. *Bioresour Technol* 2007;98:2351–68. <https://doi.org/10.1016/j.biortech.2006.10.025>.
- [19] Chiaramonti D, Buffi M, Rizzo AM, Lotti G, Prussi M. Bio-hydrocarbons through catalytic pyrolysis of used cooking oils and fatty acids for sustainable jet and road fuel production. *Biomass and Bioenergy* 2016;95:424–35. <https://doi.org/10.1016/j.biombioe.2016.05.035>.
- [20] Seifi H, Sadrameli SM. Journal of Analytical and Applied Pyrolysis Bound cleavage at carboxyl group-glycerol backbone position in thermal cracking of the triglycerides in sunflower oil. *J Anal Appl Pyrolysis* 2016;121:1–10. <https://doi.org/10.1016/j.jaap.2016.06.006>.
- [21] China 's Motor Fuels from Tung Oil 1947. <https://doi.org/10.1021/ie50456a011>.
- [22] Prado CMR, Antoniosi Filho NR. Production and characterization of the biofuels obtained by thermal cracking and thermal catalytic cracking of vegetable oils. *J Anal Appl Pyrolysis* 2009;86:338–47. <https://doi.org/10.1016/j.jaap.2009.08.005>.
- [23] Alencar JW, Alves PB, Craveiro AA. Pyrolysis of Tropical Vegetable Oils. *J Agric Food Chem* 1983;31:1268–70. <https://doi.org/10.1021/jf00120a031>.
- [24] Schwab AW, Dykstra GJ, Selke E, Sorenson SC, Pryde EH. ~ Diesel Fuel from Thermal Decomposition of Soybean Dill 2016. <https://doi.org/10.1007/BF02542382>.
- [25] Idem RO, Katikaneni SPR, Bakhshi NN. Thermal Cracking of Canola Oil: Reaction Products in the Presence and Absence of Steam 1996:1150–62. <https://doi.org/10.1021/ef960029h>.
- [26] Sadrameli SM, Aulich T, Kubátová A, Luo Y, Št J, Kozliak E, et al. New path in the thermal cracking of triacylglycerols (canola and soybean oil) 2011;90:2598–608. <https://doi.org/10.1016/j.fuel.2011.04.022>.
- [27] Asomaning J, Mussone P, Bressler DC. Journal of Analytical and Applied Pyrolysis Thermal deoxygenation and pyrolysis of oleic acid. *J Anal Appl Pyrolysis* 2014;105:1–7. <https://doi.org/10.1016/j.jaap.2013.09.005>.
- [28] Sim Y, Meyappan N, Siau N, Kamala S, Hean C, Lam W, et al. Chemical reactions in the pyrolysis of brown grease. *Fuel* 2017;207:274–82. <https://doi.org/10.1016/j.fuel.2017.06.101>.
- [29] Maher KD, Kirkwood KM, Gray MR, Bressler DC. Pyrolytic decarboxylation and cracking of stearic acid. *Ind Eng Chem Res* 2008;47:5328–36. <https://doi.org/10.1021/ie0714551>.
- [30] Shirazi Y, Viamajala S, Varanasi S. High-yield production of fuel- and oleochemical-precursors from triacylglycerols in a novel continuous-flow pyrolysis reactor. *Appl Energy* 2016;179:755–64. <https://doi.org/10.1016/j.apenergy.2016.07.025>.
- [31] Xu L, Cheng J, Liu P, Wang Q, Xu Z, Liu Q, et al. Production of bio-fuel oil from pyrolysis of plant acidified oil. *Renew Energy* 2019;130:910–9. <https://doi.org/10.1016/j.renene.2018.07.012>.
- [32] Omidghane M, Jenab E, Chae M, Bressler DC. Production of Renewable Hydrocarbons by Thermal Cracking of Oleic Acid in the Presence of Water. *Energy & Fuels* 2017;31:9446–54. <https://doi.org/10.1021/acs.energyfuels.7b00988>.
- [33] Asomaning J, Mussone P, Bressler DC. Thermal cracking of free fatty acids in inert and light hydrocarbon gas atmospheres. *Fuel* 2014;126:250–5. <https://doi.org/10.1016/j.fuel.2014.02.069>.
- [34] Mabel A, Araújo DM, Oliveira R De, Duarte A, Diniz J, Di L, et al. Thermal and catalytic pyrolysis of sun fl ower oil using AIMCM-41. *Renew Energy* 2017;101:900–6. <https://doi.org/10.1016/j.renene.2016.09.058>.
- [35] Volli V, Singh RK. Production of bio-oil from de-oiled cakes by thermal pyrolysis. *Fuel* 2012;96:579–85. <https://doi.org/10.1016/j.fuel.2012.01.016>.
- [36] Lappi H, Alén R. Journal of Analytical and Applied Pyrolysis Pyrolysis of vegetable oil soaps — Palm , olive , rapeseed and castor oils. *J Anal Appl Pyrolysis* 2011;91:154–8. <https://doi.org/10.1016/j.jaap.2011.02.003>.
- [37] Asomaning J, Mussone P, Bressler DC. Pyrolysis of polyunsaturated fatty acids. *Fuel Process Technol* 2014;120:89–95. <https://doi.org/10.1016/j.fuproc.2013.12.007>.
- [38] Asomaning J, Mussone P, Bressler DC. Two-stage thermal conversion of inedible lipid

-
- feedstocks to renewable chemicals and fuels. *Bioresour Technol* 2014;158:55–62. <https://doi.org/10.1016/j.biortech.2014.01.136>.
- [39] Sadrameli SM, Green AES. Systematics of renewable olefins from thermal cracking of canola oil 2007;78:445–51. <https://doi.org/10.1016/j.jaap.2006.12.010>.
- [40] Meier HF, Wiggers VR, Zonta GR, Scharf DR, Simionatto EL, Ender L. A kinetic model for thermal cracking of waste cooking oil based on chemical lumps. *Fuel* 2015;144:50–9. <https://doi.org/10.1016/j.fuel.2014.12.020>.
- [41] Fimberger J, Swoboda M, Reichhold A. Thermal cracking of canola oil in a continuously operating pilot plant. *Powder Technol* 2017;316:535–41. <https://doi.org/10.1016/j.powtec.2016.10.030>.
- [42] Biswas S, Sharma DK. Journal of Analytical and Applied Pyrolysis Studies on cracking of *Jatropha* oil. *J Anal Appl Pyrolysis* 2013;99:122–9. <https://doi.org/10.1016/j.jaap.2012.10.013>.
- [43] Shim J, Jeon K, Jang W, Na H, Cho J, Kim H. Applied Catalysis B: Environmental Facile production of biofuel via solvent-free deoxygenation of oleic acid using a CoMo catalyst. *Appl Catal B Environ* 2018;239:644–53. <https://doi.org/10.1016/j.apcatb.2018.08.057>.
- [44] Liu Y, Yang X, Liu H, Ye Y, Wei Z. Applied Catalysis B: Environmental Nitrogen-doped mesoporous carbon supported Pt nanoparticles as a highly efficient catalyst for decarboxylation of saturated and unsaturated fatty acids to alkanes. *Applied Catal B, Environ* 2017;218:679–89. <https://doi.org/10.1016/j.apcatb.2017.06.065>.
- [45] Idem RO, Katikaneni SPR, Bakhshi NN. Catalytic conversion of canola oil to fuels and chemicals: roles of catalyst acidity, basicity and shape selectivity on product distribution. *Fuel Process Technol* 1997;51:101–25. [https://doi.org/10.1016/S0378-3820\(96\)01085-5](https://doi.org/10.1016/S0378-3820(96)01085-5).
- [46] Charles Mortimer Chemistry VI Edition.pdf n.d.
- [47] Zanichelli. *Energie di Legame e ΔH di Reazione* 2012;3:1–8.
- [48] Garzanti. *Chimica* 2018.
- [49] Università di Bologna. *Proprietà Fisiche Dei Composti Organici* 1998;34:466–70.
- [50] Università di Roma. *Il Legame Chimico* n.d.
- [51] Università di Venezia. *Modulo 05: legami, molecole e reazioni* 2019:3–6.
- [52] Periyasamy B. Reaction pathway analysis in thermal cracking of waste cooking oil to hydrocarbons based on monomolecular lumped kinetics. *FUEL* 2015;158:479–87. <https://doi.org/10.1016/j.fuel.2015.05.066>.
- [53] Lappi H, Ale R. Journal of Analytical and Applied Pyrolysis Production of vegetable oil-based biofuels — Thermochemical behavior of fatty acid sodium salts during pyrolysis 2009;86:274–80. <https://doi.org/10.1016/j.jaap.2009.07.005>.
- [54] FORGE Hydrocarbons Corp n.d.
- [55] ASTM. Standard Test Methods for Instrumental Determination of Carbon, Hydrogen, and Nitrogen in Petroleum Products and Lubricants D5291 – 10. ASTM. West Conshohocken, PA (USA): American Society for Testing and Materials: 2011.
- [56] ASTM. Standard Test Method for Trace Nitrogen in Liquid Petroleum Hydrocarbons by Syringe/Inlet Oxidative Combustion and Chemiluminescence Detection ASTM D4629. ASTM, West Conshohocken, PA (USA): American Society for Testing and Materials: 2011.
- [57] DIN. Determining the gross calorific value of solid and liquid fuels using the isoperibol or static-jacket calorimeter, and calculation of net calorific value. DIN 51900-2. DIN. Beuth Verlag GmbH, 10772 Berlin, Germany, Deutsches Institut Für Normung e.V.: 2003.
- [58] CEN. Determining the gross calorific value of solid and liquid fuels using the bomb calorimeter, and calculation of net calorific value. DIN 51900-1. DIN. Beuth Verlag GmbH, 10772 Berlin, Germany, Deutsches Institut Für Normung e.V.: 2000.
- [59] CEN. Determining Animal and vegetable fats and oils. Determination of acid value and acidity. EN ISO 660. Brussels, Belgium: European Committee for Standardization: 2009.
- [60] CEN. Fat and oil derivatives - Fatty Acid Methyl Esters (FAME) - Determination of acid value EN 14104. Brussels, Belgium: European Committee for Standardization: 2003.

-
- [61] CEN. Determination of kinematic viscosity and calculation of dynamic viscosity of transparent and opaque liquids DIN EN ISO 3104. Brussels, Belgium: European Committee for Standardization: 1996.
- [62] CEN. Animal and vegetable fats and oils. Determination of water content Karl Fischer method (pyridine free) EN ISO 8534. Brussels, Belgium: European Committee for Standardization: 2008.
- [63] Oasmaa A, Peacocke C. Properties and fuel use of biomass-derived fast pyrolysis liquids. A guide. vol. 731. 2010.
- [64] CEN. Liquid petroleum products –Determination of contamination in middle distillates DIN EN 12662. Brussels, Belgium: European Committee for Standardization: 2008.
- [65] CEN. Crude petroleum and liquid petroleum products. Laboratory determination of density. Hydrometer method EN ISO 3675. . . Brussels, Belgium: European Committee for Standardization: 2008.
- [66] CEN. Petroleum products - Determination of ash. EN ISO 6245. Brussels, Belgium: European Committee for Standardization: 2002.
- [67] CEN. Animal and vegetable fats and oils.Preparation of methyl esters of fatty acids EN ISO 5509. ISO. CaBrussels, Belgium: European Committee for Standardization: 2000.
- [68] Reaume SJ. Cold flow improvements to biodiesel through the use of heterogeneous catalytic skeletal isomerization 2013.
- [69] Guedes RE, Luna AS, Torres AR. Journal of Analytical and Applied Pyrolysis Operating parameters for bio-oil production in biomass pyrolysis : A review. J Anal Appl Pyrolysis 2018;129:134–49. <https://doi.org/10.1016/j.jaap.2017.11.019>.